Discovery of Potent Kappa Opioid Receptor Agonists Derived from Akuammicine

Madeline R. Hennessy[1], Simone M. Creed[1], Anna M. Gutridge[2], Elizabeth S. Rhoda[2], Richard M. van Rijn[2-5], Andrew P. Riley[1]*

[1] Department of Pharmaceutical Sciences, College of Pharmacy, University of Illinois Chicago, Chicago, IL 60612 USA, [2] Department of Medicinal Chemistry and Molecular Pharmacology, College of Pharmacy, Purdue University, West Lafayette, IN 47907 USA, [3] Purdue Institute for Drug Discovery, [4] Purdue Institute for Integrative Neuroscience, [5] Purdue Interdisciplinary Life Sciences Graduate Program, Purdue University, West Lafayette, IN 47907 USA

ABSTRACT

Akuammicine (**1**), an indole alkaloid isolated from the seeds of *Picralima nitida*, is a selective agonist of the kappa opioid receptor (κOR). To establish structure-activity relationships (SAR) for this structurally unique κOR ligand, a collection of 26 semisynthetic derivatives of **1** were synthesized. Evaluating these derivatives for their ability to activate the κOR and mu opioid receptor (μOR) revealed key SAR trends and identified derivatives with enhanced κOR potency. Most notably, substitutions to the C10 position of the aryl ring led to a >200-fold improvement in κOR potency and nearly complete selectivity for the κOR over other CNS receptor targets. Activation of the κOR by these analogues also results in the recruitment of β-Arrestin-2, indicating they are balanced agonists and have distinct signaling properties from other recently identified κOR agonists. The discovery of these κOR agonists underscores the potential of using natural products to identify new classes of highly potent and selective ligands and provides new pharmacology tools to probe the κOR.

INTRODUCTION

The mu, kappa, delta, opioid receptors (μOR, κOR, and δOR) and the nociception receptor (NOR) make up the opioid receptor family of G-protein coupled receptors (GPCRs).[1] The opioid receptors are distributed throughout the peripheral and central nervous systems (CNS), where they participate in pain processing, mood, reward, and stress.[2] Although all opioid receptors play a significant role in pain sensation, most clinically used opioid analgesics, like morphine and fentanyl, derive their effects via activation of the μOR.[1,3] However, the addictive properties of opioid analgesics, and the opium from which they are derived, is infamous and was well appreciated even before their implementation as medicine.[4–6] Moreover, the serious, sometimes life-threatening adverse effects of μOR agonists, including sedation, respiratory depression, tolerance, and constipation significantly diminishes their safety, particularly when used chronically.[2] Additionally, many patients prescribed opioids voluntarily discontinue their opioid therapy due to their severe side effects; however, discontinuation of opioids may provoke withdrawal symptoms that require additional treatments.[7]

In light of these issues, the κOR system has been proposed as a potential target for developing safer, less-addictive drugs.[8–10] *In vivo*, κOR agonists produce analgesic and anti-pruritic effects, but lack the addictive properties and adverse effects of μOR agonists. Furthermore, κOR agonists have also been investigated in a range of other therapeutic areas including substance use disorders, multiple sclerosis, and ischemia.[11] Driven by the therapeutic potential of the κOR, several structurally diverse classes of κOR agonists have been discovered and developed including the arylacetamides, morphinans, diterpenes, triazoles, and synthetic peptides (**Figure 1**).[12–18]

Figure 1. Representative scaffolds of κOR ligands.

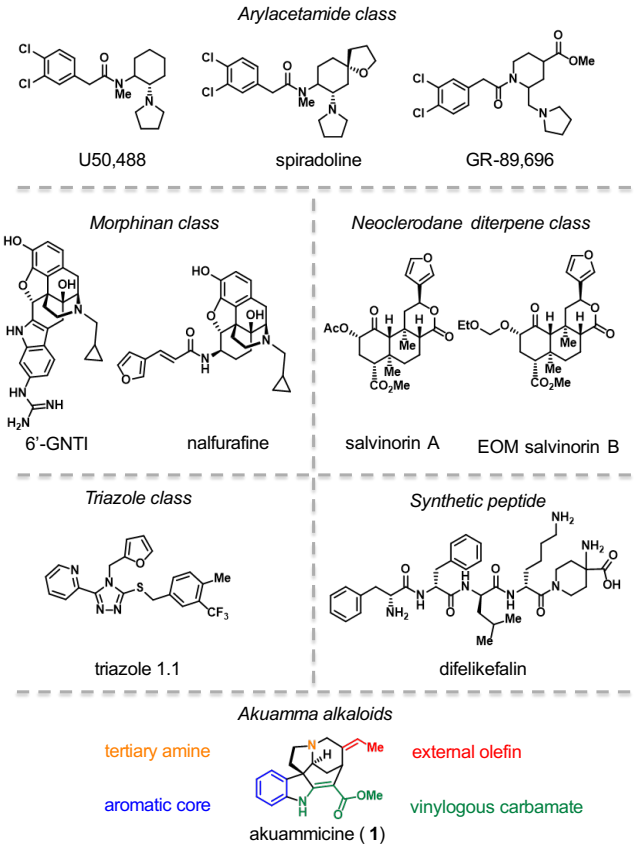

Although these κOR agonists lack the abuse potential and respiratory depression of μOR agonists, many κOR agonists produce severe sedation, dysphoria, and psychotomimetic effects.[19–21] Until the very recent approval of nalfurafine and difelikefalin as anti-pruritic agents, these κOR-dependent side effects have prevented the use of κOR agonists in the clinic.[22,23] As such, considerable effort has been made to understand the biological mechanisms through which κOR agonists produce their behavioral effects. It is now generally accepted that the anti-pruritic and analgesic effects arise from the canonical G-protein-mediated signaling cascades, wherein the binding of a κOR agonist induces a conformational change in the receptor that leads to dissociation of the G_α and G_β/G_γ subunits, which in turn interact with downstream signaling effectors.[24] Conversely, the underlying mechanism responsible for the adverse effects has not been as firmly established. Early work by the Chavkin lab suggested that the dysphoria and

aversion of κOR were dependent on G-protein-coupled receptor kinase 3 (GRK3) and p38 activation mediated through the recruitment of βArrestin-2 (βArr2) to the receptor.[24–28] Similarly, the ability of a ligand to recruit βArr2 has also been correlated with sedation in mice.[12] The association between βArr2 recruitment and κOR adverse effects has spurred the investigation of so-called G-protein biased agonists that preferentially activate G-protein signaling without inducing βArr2 recruitment.[29,30] However, conflicting studies have shown that κOR agonists still produce aversion in βArr2-knockout mice, which suggests βArr2 is not required.[31] Moreover, while several classes of biased agonists have been identified, it is unclear what degree of G-protein bias is necessary to produce a therapeutically meaningful reduction in adverse effects. Furthermore, although advances in cryogenic electron microscopy (cryo-EM) have provided several recent structures of the κOR bound to agonists with different levels of bias, our ability to predict and control a ligand's ability to activate discreet signaling cascades remains limited.[32] Thus, given the uncertainty surrounding the mechanism responsible for the κOR-dependent adverse effects and the challenges associated with designing agonists with specific signaling properties, the discovery of novel, high potency agonist remains an important tool in studying the κOR.

With classic examples like morphine, and more recently salvinorin A and mitragynine, natural products have historically served as excellent sources of pharmacological probes to study the opioid receptors.[33,34] Looking to add to this body of work, our group recently characterized several alkaloids found in the seeds of the akuamma tree with moderate affinity for the opioid receptors.[35,36] In particular, akuammicine (**1**) was found to bind and activate the κOR preferentially over the μOR and δOR. Notably, the monoterpene indole alkaloid scaffold of **1** is structurally distinct from other κOR ligands. These features may allow **1** and its derivatives to engage the κOR in unique ways and produce pharmacological profiles distinct from existing κOR agonists. To test this hypothesis and investigate the structure-activity relationship (SAR) of **1**, a series of 26 derivatives were synthesized and evaluated for activity at the opioid receptors. In addition to establishing the first SAR trends of **1**, these studies identified modifications that led to a

dramatic >200-fold improvement in κOR potency and >800-fold selectivity over other receptors and targets.

RESULTS

Chemistry

To begin our SAR studies, we recognized that **1** contained four apparent functional groups capable of making ligand-receptor interactions with the κOR (**Figure 1**): (1) the aromatic core, (2) the external olefin appended at C19, (3) the vinylogous carbamate, and (4) the tertiary nitrogen. To investigate the nature of these potential interactions, a series of highly chemoselective reactions were employed to modify these sites on **1**. To begin these studies **1** was isolated from commercial *P. nitida* seeds and purified using a pH-zone refining counter-current chromatography as previously described.[35]

C10 modifications

The modification of the aromatic core began with the acid-mediated halogenation of **1** with *N*-bromo succinimide (NBS) and *N*-iodo succinimide (NIS), which exclusively produced 10-bromo akuammicine (**2**) and 10-iodo akuammicine (**3**) (**Scheme 1**).[37] In addition to introducing additional steric bulk, lipophilicity, and potential for halogen-bonding interactions, these aryl halides also serve as excellent functional handles to install substitutions to probe the κOR binding pocket. For instance, furan rings exist in numerous κOR ligands, including nalfurafine, salvinorin A, and triazole 1.1, suggesting this heterocycle may represent a privileged scaffold for the κOR. Fortunately, **3** demonstrated to be a competent coupling partner with aryl and heterocyclic boronic acids to produce analogues **4**-**6**.[38]

Scheme 1. Modification of the C10 position of akuammicine (**1**)[a]

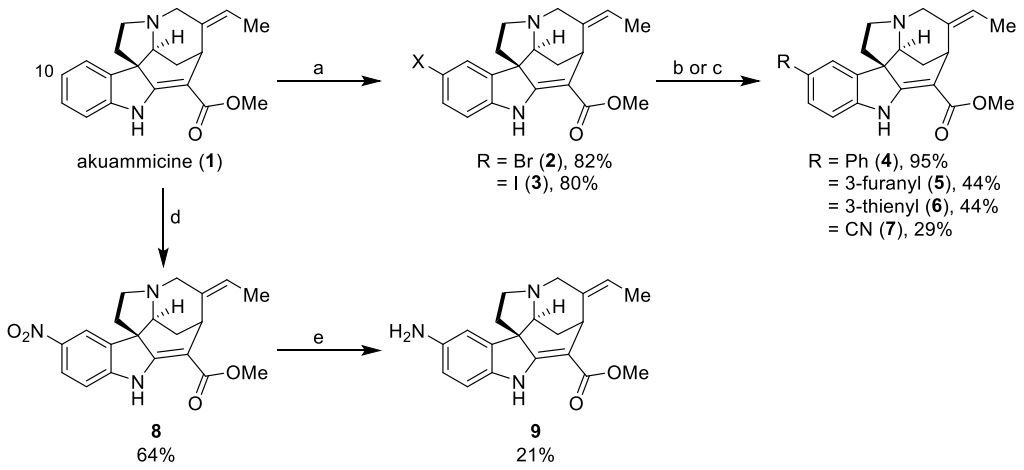

[a]*Reagents and conditions*: (a) NXS, DCM/TFA (1:1), 0°C, 4 h; (b) from **3**, K_2CO_3, R–$B(OH)_2$, $Pd(PPh_3)_4$, PhMe/MeOH (3:2), 80°C, 3-4 h; (c) from **2**, $Zn(CN)_2$, Pd G3 ^{t}BuXPhos, 1,4-dioxane/H_2O (1:3), 85°C, 12-18 h (**d**) HNO_3, DCM, rt, 15 min; (**e**) $SnCl_2$, EtOH, 70°C 2-4 h.

Further C10 modifications were pursued to probe the effect of appending electron-withdrawing and electron-donating groups on the aromatic ring. Palladium-catalyzed cyanation afforded the 10-cyanoakuammicine (**7**).[39] Additionally, nitration of **1** exclusively afforded the 10-nitroakuammicine (**8**), further illustrating a strong preference for electrophilic aromatic substitution to occur at the C10 position of **1**. Reduction of **8** with stannous chloride produced the corresponding aryl amine **9**. Although **9** is a useful counterpoint to the electron-poor rings in **7** and **8**, and introduces potential hydrogen-bonding interactions, the low yields of this reduction and difficulties in its purification prevented its use as a synthetic intermediate for further modification.

C2,16 and C19,20 olefin modifications

Alstolucines A-F are a small family of alkaloids isolated from *Alstonia spatulata* that bear the same pentacyclic framework as **1**, but with oxidized side chains in place of the C19,20 olefin.[40] Despite this structural similarity to **1**, the pharmacological activity of the alstolucines at the κOR has not been assessed. To explore how additional polarity at this position would influence opioid activity, we employed a similar route originally developed by the Andrade group to oxidize the

external olefin of **1**.[40] Upjohn dihydroxylation of the C19,20 olefin of **1** yielded the diastereomeric *syn*-diol products **10** and **11** in a 9:1 ratio with the major product, **10**, arising from the addition of osmium tetroxide to the convex side of **1** (**Scheme 2**).[40] Notably, **11** was not originally reported by Andrade, likely due to fact it is produced in low yield. Swern oxidation of the secondary alcohol in **10** produced the ketone **12**.[40]

In addition to introducing hydrogen bond donors and acceptors, the exocyclic olefin in **1** also introduces a stereogenic center at C20 and flexibility in the C18-C19 bond. In an attempt to separate steric effects from the polar effects of the oxygens in **10**-**12**, we also reduced the olefin with platinum (IV) oxide to yield 19,20-dihydroakuammicine (**13**).[40–42] As noted by Andrade, this reduction is both stereoselective and chemoselective, producing **13** as a single diastereomer and no apparent reduction of the vinylogous carbamate. Exposure of **1** or **13** to sodium cyanoborohydride selectively reduced the C2,16 internal olefin to produce the 2,16-dihydroakuammicine (**14**) and 2,16,19,20-tetrahydroakuammicine (**15**), respectively (**Scheme 2**).[41]

Scheme 2. Oxidation and reduction of akuammicine (**1**) olefins [a]

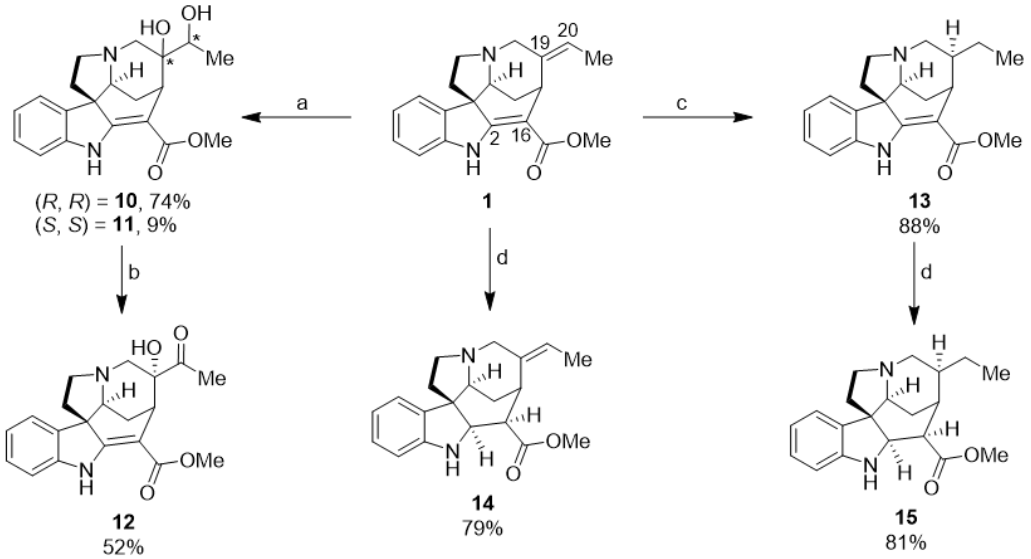

[a]*Reagents and conditions*: (a) NMO, OsO_4, $^tBuOH/THF/H_2O$ (3:2:1), rt, 12-18 h; (b) from **10**, DMP, H_2O, DCM, rt, 3 h; (c) PtO_2 (10% wt.), MeOH, rt, 8 h; (d) $NaCNBH_3$, $AcOH/H_2O$ (3:2), 0 °C, 4 h.

N4 alkylation

On the morphinan scaffold μOR antagonists such as naloxone and naltrexone typically feature allyl and cyclopropyl methyl appendages on the tertiary nitrogen, whereas agonists such as morphine and oxycodone have a methyl group at this position.[43,44] Additionally, methylation of the tertiary amine, for example as seen in gut motility agent methylnaltrexone, has proven to be an effective strategy for peripherally restricting morphine-derived opioids while maintaining affinity for the receptor.[45] To see whether similar trends apply to **1**, the tertiary amine was alkylated with the corresponding alkyl halide to introduce a methyl, propyl, allyl, methyl cyclopropyl, and benzyl group (**Scheme 3**). Because **16**-**20** bear quaternary amines, their purification using normal phase silica gel chromatography proved challenging. Instead, a modified ion exchange column using silica gel presaturated with a methanolic solution of sodium bromide was used to purify the alkyl derivatives as bromide salts.[46]

Scheme 3. Synthesis of quaternary amines of akuammicine (**1**)[a]

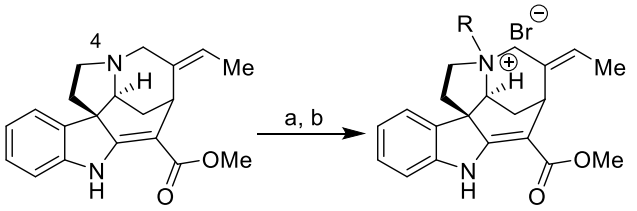

R = Me (**16**), 16%
= *n*-propyl (**17**), 90%
= allyl (**18**), 83%
= CH_2-*c*-propyl (**19**), 80%
= benzyl, (**20**), 88%

[a]*Reagents and conditions*: (**a**) R-Br or R-I, $CHCl_3$, 60 °C, 1-4 h; (**b**) NaBr-impregnated silica gel.

Doubly substituted derivatives

An initial pharmacological characterization of the C10-substitited, olefin-modified, and *N*-alkylated derivatives revealed that C10 halogenation led to significant increases in κOR potency

(*vide infra*). Based on this observation, we also prepared a series of halogenated derivatives that contain modifications to the olefins or tertiary amine (**21**-**27**, **Scheme 4**).

Scheme 4. Synthesis of doubly modified derivatives. [a]

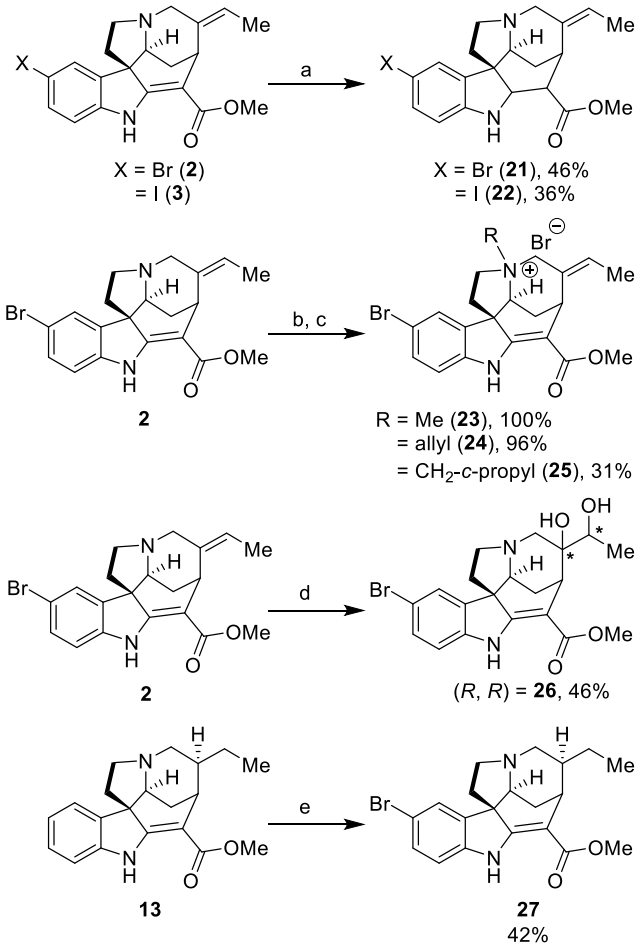

[a]*Reagents and conditions*: (a) $NaCNBH_3$, $AcOH/H_2O$, 0 °C, 4 h; (b) R-Br, $CHCl_3$, 60 °C, 1-4 h; (c) R-I, $CHCl_3$, NaBr, 60 °C, 1-4 h; (d) NMO, OsO_4, $^tBuOH/THF/H_2O$ (3:2:1), rt, 12-18 h; (e) NBS, TFA, DCM, 0 °C, 4 h.

Employing similar conditions to those described above to modify **1**, reduction of the C2,16 olefin of halogenated analogues **2** and **3** selectively produced analogues **21** and **22** as single diastereomers. The *N*-alkylation procedure was similarly adapted to yield analogues **23**-**25** from **2**. However, the Upjohn dihydroxylation of **2** produced considerably lower yields compared to that of **1**. As a result, only the major product (**26**) could be isolated in sufficient amounts for evaluation.

Finally, concerned that the reduction of the C19,20 olefin with PtO_2 would also result in protodehalogenation, we opted to brominate **13** to synthesize **27**.

***In vitro* pharmacology**

Having generated a collection of 26 akuammicine analogues with modifications to the C10 (**2**-**9**), C19,20 (**10**-**13**, **15**, **26**, **27**), C2,16 (**14**, **21**, **22**) and *N*4 (**16**-**20**, **23**-**25**) positions, we looked to examine how these modifications would impact opioid receptor activity. Because our previous studies indicated the akuamma alkaloids are moderately potent κOR and μOR agonists with negligible activity at the δOR, all compounds were first evaluated at the κOR and μOR using a cell-based system that measured inhibition of forskolin-induced production of cAMP as a measure of G-protein pathway activation (**Table 1**).[35,36] Notably, consistent with our initial characterization of **1** as a selective κOR agonists, except in instances where the modifications removed all agonist activity, the derivatives were full κOR agonists with considerably greater potency at the κOR than the μOR. And while most of these derivatives possess similar efficacies, it was noted that several modifications had considerable effects on the compounds' potency at the κOR.

Table 1. Inhibition of cAMP by analogues of **1** at the κOR and the μOR

	κOR cAMP inhibition[a]			μOR cAMP inhibition[a]		
Compound	**pEC_{50} ± SEM[b]**	**EC_{50} (nM)**	**Emax (%) ± SEM[b]**	**pEC_{50} ± SEM[b]**	**EC_{50} (nM)**	**Emax (%) ± SEM[b]**
U50,488	9.0 ± 0.1	0.98	100 ± 2	--	--	--
DAMGO	--	--	--	9.2 ± 0.1	0.6	100 ± 2
1	5.9 ± 0.1	1200	91 ± 7	--	--	<10%
2	8.4 ± 0.1	3.9	96 ± 2	5.0 ± 0.9	11000	62 ± 64
3	8.2 ± 0.1	5.7	98 ± 2	4.4 ± 1.9	41000	<10%
4	7.8 ± 0.1	15	101 ± 2	6.1 ± 0.1	780	106 ± 6
5	9.1 ± 0.1	0.88	102 ± 2	6.1 ± 0.2	720	99 ± 12
6	8.1 ± 0.1	7.7	104 ± 3	6.1 ± 0.1	840	107 ± 3
7	7.1 ± 0.2	81	102 ± 6	--	--	<10%
8	6.8 ± 0.1	160	96 ± 5	5.4 ± 0.8	4000	<10%
9	6.6 ± 0.1	260	107 ± 5	--	--	<10%
10	--	--	<10%	--	--	<10%
12	--	--	<10%	--	--	<10%
13	5.8 ± 0.1	1600	99 ± 9	--	--	<10%
14	--	--	<10%	--	--	<10%
15	--	--	<10%	--	--	<10%
16	--	--	<10%	--	--	<10%
17	--	--	<10%	--	--	<10%
18	--	--	<10%	--	--	<10%
19	5.3 ± 0.3	4700	113 ± 24	--	--	<10%
20	--	--	<10%	5.6 ± 0.1	2300	112 ± 6
21	7.3 ± 0.1	47	100 ± 4	--	--	<10%
22	7.6 ± 0.1	24	100 ± 5	--	--	<10%
23	6.0 ± 0.1	940	102 ± 7	--	--	<10%
24	6.2 ± 0.1	650	100 ± 7	--	--	<10%
25	6.7 ± 0.1	210	94 ± 5	--	--	<10%
26	--	--	<10%	--	--	<10%
27	7.5 ± 0.1	31	100 ± 5	6.0 ± 0.1	1100	107 ± 5

[a]cAMP inhibition at the κOR and the μOR was determined through the HitHunter assay.
[b]Mean ± standard error on the mean from a minimum of three independent assays.
-- = no activity observed at 10 μM.

C10 modifications

The most dramatic increase in κOR potency was observed in compounds bearing substitutions to the C10 position of the aromatic ring. Compounds **2** and **3** with a bromine and iodine at this position are potent κOR agonist (EC_{50} = 3.9 and 5.7 nM), representing a >300- and 200-fold increase in potency relative to **1** (**Figure 2B**, **Table 1**). Despite this striking increase in potency elicited by a single atom substitution, this effect appears to be specific to the κOR and **2** and **3** only weakly activated the μOR thereby maintaining >2,800-fold selectively for the κOR over the μOR (**Figure 2 D**, **Table 1**). Similar trends were also observed when the affinity of **2** and **3**

were measured at the κOR and μOR using a radioligand displacement assay (**Figure 2A-B**, **Table S1**). Compounds **2** and **3** tightly bind to the κOR (K_i = 0.36 nM and 0.087 nM, respectively) and have 15,000- and 40,000-fold greater affinity for the κOR over the μOR.

Figure 2. Pharmacological characterization of the akuammicine (**1**) analogues **2**-**6** and **8** at the μOR and κOR.

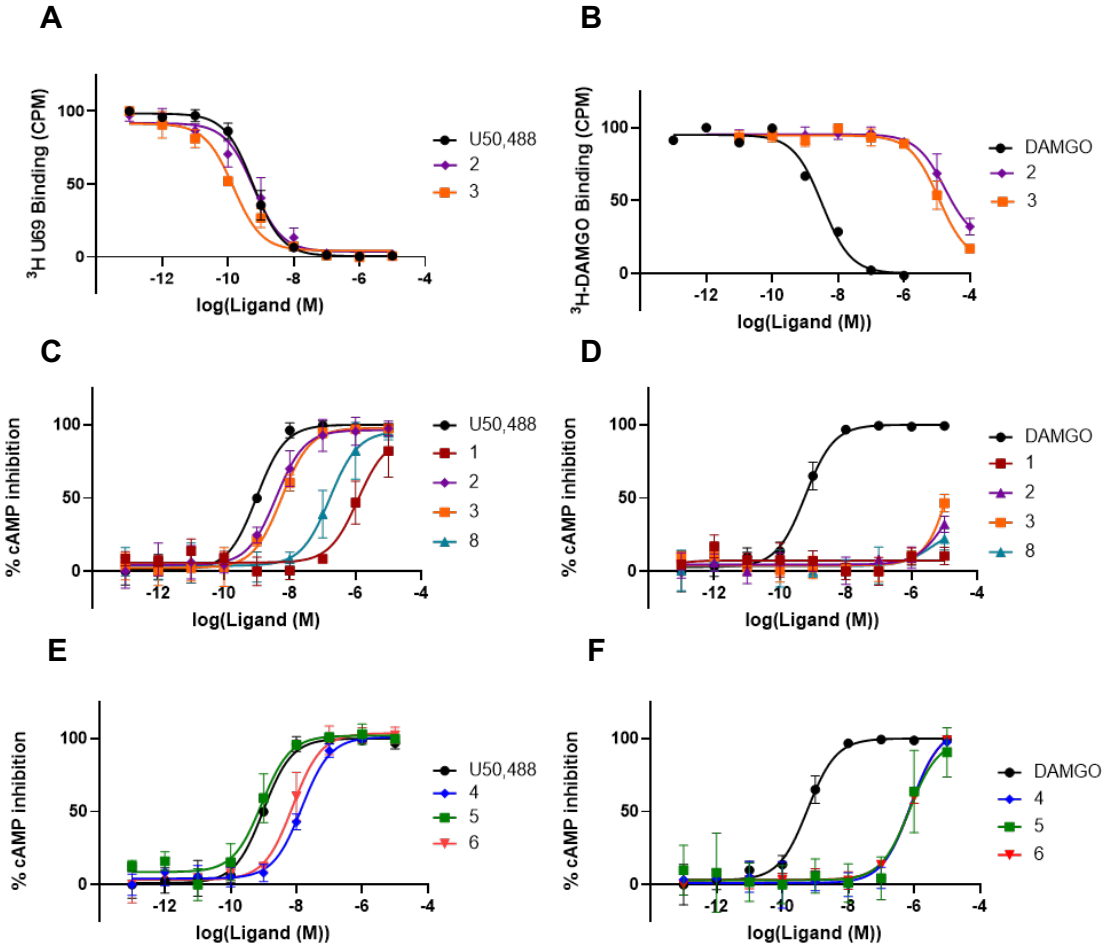

Compounds **2** and **3** were screened radioligand binding assay at the κOR and μOR using [^{3}H]U69,593 and [^{3}H]DAMGO, respectively (**A** and **B**). Inhibition of forskolin-induced cAMP of **1**-**6** and **8** in a HitHunter assay at the κOR (**C** and **E**) μOR (**D** and **F**). All curves are representative of the averaged values from a minimum of three independent assays.

Functionalization of the C10 position of **1** with the phenyl (**4**), 3'-furanyl (**5**), and 3'-theinyl (**6**) moiety also elicited a significant effect on κOR and μOR potency (**Figure 2E-F**). Analogue **4** activated the κOR more potently than **1** (EC_{50} = 15 nM). Likewise, compound **5** activated the

κOR >1,300 times more potently than the parent compound **1** (EC_{50} = 0.88 nM). Notably, **5** was the most potent analogue identified and possesses similar potency as the control agonist U50,488 (**Table 1**). Moreover, analogue **6** also potently activates the κOR (EC_{50} = 7.7 nM). Unlike the halogenated derivatives, compounds **4**-**6** do activate the μOR (EC_{50} 720-840 nM) and thus have less selectivity for the κOR than **2** and **3**.

Installation of the nitrile (**7**) to the C10 position also modulated κOR activity (EC_{50} = 81 nM) without activating the μOR. A similar effect as **7** on κOR potency was observed with the C10 nitro analogue (**8**), most likely due to their similar electron-withdrawing capabilities. However, compared to **7**, analogue **8** has slightly reduced κOR potency (EC_{50} = 160 nM) and does weakly activate the μOR (EC_{50} = 4,000 nM) (**Figure 2C**-**D**). It is worth noting that the improved potency of C10-substituted derivatives does not appear to be limited to electron-withdrawing substituents as the aryl amine **9**, also possess increased κOR potency (EC_{50} = 260 nM) compared to **1**.

Olefin oxidation and reduction

While substitutions at C10 appear to improve κOR potency, changes to the olefins were generally less well-tolerated (**Table 1**). Compounds **10** and **12** bearing olefin oxidations possess no agonist activity at either the κOR or μOR. Conversely, reduction of the C19,20 olefin (**13**) did not have a considerable impact on κOR potency (EC_{50} = 1,600 nM), producing a similar agonist effect as the natural product **1**. Because the ethyl group of **13** appears to be tolerated, the reduced activity of **10** and **12** is likely due to the additional polarity introduced by the oxygens, rather than forcing the ethyl group into an unfavorable position within the κOR binding site. As opposed to the external olefin, when the C2,16 olefin is reduced (**14** and **15**) all κOR agonist activity is abolished or significantly diminished. This might suggest that the vinylogous carbamate is required for κOR activation and perhaps even serving as an electrophilic site to covalently bind to the κOR. However, analogues **21** and **22** bearing halogens at the C10 of **15** do have κOR activity (EC_{50} = 47 and 24 nM, respectively). Instead, it is more likely that breaking the extended system

of conjugation between the ester and the arylamine forces the ester into an orientation that makes less favorable interactions with the κOR. Interestingly, halogenation of the C10 position is not sufficient to rescue the activity of **10** (**26**), which further supports the notion that the exocyclic olefin most likes points into a small hydrophobic pocket where small, non-polar functionalities are not tolerated.

N4 alkylation

Generally, alkylation of the tertiary nitrogen of **1** was detrimental to opioid activity. The alkylated analogues **16**-**18** and **20** have no agonistic activity at the κOR or μOR; however, the cyclopropylmethyl analogue **19**, did produce κOR agonistic activity (EC_{50} = 4,700 nM) albeit with about 4-fold reduced potency compared to **1**. Introduction of a bromine atom at C10 once again rescues the agonist activity of the *N*4-alkylated analogues (**23**-**25**). While these alkylated analogues are considerably less potent than **2** (EC_{50} = 210-940 nM), they did surpass the potency of the parent natural product **1**. Additionally, the potency of the C10 brominated, N4 alkylated analogues increased as the steric bulk of the alkylation increased (cPr > allyl > Me), suggesting the N4 alkyl substituents may be reaching into a hydrophobic pocket of the κOR.

*Additional In Vitro Characterization of **2** and **3***

Given the striking increase in potency **2** and **3** at the κOR in the HitHunter cAMP inhibition assay, while maintaining a high degree of selectivity over the μOR, the opioid receptor signaling of these analogues were further examined. As discussed, several early studies have hypothesized that G-protein biased κOR agonists are less aversive and sedative than balanced agonists.[12,47,48] Therefore, we first evaluated the ability of **2** and **3** to induce βArr2 recruitment using the PathHunter assay. Previously, we have shown that the natural product **1** only recruits βArr2 at the κOR at high doses (EC_{50} = 39 μM), preventing us from calculating a bias factor.[35] However, in addition to having increased G-protein potencies, **2** and **3** more potently induce βArr2

recruitment at the κOR with similar potency as the reference ligand U50,488 (**Figure 3**). As a result, compounds **2** and **3** represent a novel class of potent κOR agonists with a G-protein/βArr2-balanced signaling profile.

Figure 3. β-Arrestin-2 (βArr2) recruitment of analogues **2** and **3** at the κOR.

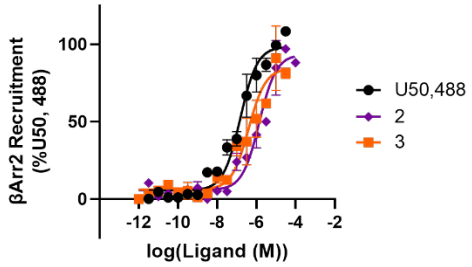

κOR β-Arrestin-2 Recruitment[a]				
	pEC_{50} ± SEM[b]	EC_{50} (nM)	Emax (%) ± SEM[b]	Bias factor[c]
U50,488	6.82 ± 0.1	150	93 ± 4	--
2	5.85 ± 0.1	1400	88 ± 7	0.34
3	6.40 ± 0.2	400	78 ± 6	-0.38

[a]Recruitment of βArr2 in a PathHunter assay at κOR of **2** and **3** with U50,488 as a control. [b]Mean ± standard error on the mean from a minimum of three independent assays. [c]The degree of ligand bias was calculated through intrinsic relative activity.[49]

Previous reports by our lab demonstrated that the natural product **1** displays affinity towards a plethora of CNS targets, albeit at considerably lower affinity than it binds to the κOR[35]. Because **2** and **3** have increased κOR affinity, we sought to determine whether these modifications at the C10 position would also improve selectivity. To do so, **2** and **3** were screened for affinity against a panel of 54 GPCRs, ion channels, and transporters by the Psychoactive Drug Screening Program (PDSP). An initial radioligand binding screen at a single concentration of 10 μM of each analogue was performed to identify potential off-target receptor affinity (**Table S2**). In instances where **2** or **3** displaced >50% of radioligand from an off-target, multidose concentration-response curves were generated to calculate binding affinity (K_i) (**Table 3**). In comparison to the natural product **1**, compounds **2**, and **3** exhibit binding affinities at an increased number of targets namely the serotonin receptors and adrenergic receptors. However, **2** and **3** possess relatively

weak affinity for these off-targets and have >200-fold greater affinity for the κOR over all off-targets investigated, including the μOR and δOR, indicating they are highly selective κOR ligands.

Table 2. Binding affinities (K_i) of **1**-**3** at CNS receptors and transporters.[a]

	1[b]	2	3
Receptor	**K_i (nM)**	**K_i (nM)**	**K_i (nM)**
KOR	166	1	1
MOR	3729	--	--
5-HT2A	4822	--	2314
5-HT2A	--	--	--
5-HT2B	--	1794	767
5-HT2B	--	--	--
5-HT3	5494	210	384
5-HT5A	2931	721	829
5-HT7A	1408	1515	1385
Alpha1A	--	1004	883
Alpha1B	--	2877	2017
Alpha1D	--	--	1140
Alpha2A	--	> 10,000	732
Alpha2B	1214	1249	--
Alpha2C	4794	2909	2864
Alpha7	--	6999	5488
HERG	--	1342	1102
NET	--	--	3436
Sigma 2	--	2625	2218

[a]Binding affinities were determined through the Psychoactive Drug Screening Program (PDSP) utilizing radioligand displacement assays through an average of three independent trials. "–" indicates compound produced less than 50% displacement of radioligand in primary binding screen at 10 μM. [b]Data from reference 35.

To further probe their selectivity, **1**-**3** were screened for functional activity against the GPCRome using a PRESTO-Tango assay that measures βArr2 recruitment to a large panel of GPCRs. Remarkably, **1**-**3** possess nearly complete selectivity for the κOR and caused very little recruitment of βArr against the 320 non-olfactory GPCRs evaluated (**Figure 4**). Interestingly, the atypical chemokine receptor CXCR7, which was identified as a potential target of **3**, was also identified as putative target for the indole alkaloid conolidine and metabolites of the indole alkaloid mitragynine.[50,51] Moreover, CXCR7 is expressed in the same brain regions as the opioid receptors and is believed to be responsible for scavenging opioid peptides.[52] Thus, CXCR7 appears to be

a common target for opioid ligands, especially indole alkaloids. Although, it is intriguing that **2** does not appear to possess this same effect and fails to induce βArr recruitment at CXCR7.

Figure 4. GPCRome screening of compounds **1**, **2**, and **3** using the Presto-Tango Assay.

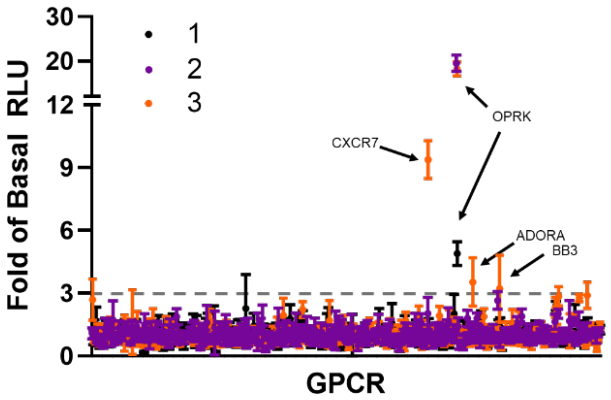

Data collected by the PDSP using PRESTO-Tango to measure βArr2 recruitment at 3 μM. Compounds 1-**3** were screened at 320 non-olfactory GPCRs βArr2 for agonism. Data is presented as the fold-change from basal relative luminesce units (RLUs) from an average of three assays. GPCRs which induced >3-fold change are labeled while a comprehensive list of GPCRs is reported previously.[53]

Discussion

The seeds of the akuamma tree have been used as an ethnomedicine in its native West Africa for its pain-relieving effects.[54,55] These analgesic effects have generally been attributed to the μOR-selective indole alkaloids akuammine and pseudo-akuammigine.[35,56–58] However, the presence of **1**, a selective κOR agonist, also suggests activity at this receptor may be contributing to the observed physiological effects of akuamma seeds.[59,60] Indeed, the utility of the κOR as a safer target for pain relief has been explored due to its ability to produce analgesic effects without the addictive properties seen with μOR agonists.[8–10] Moreover, because **1** is structurally distinct from previously investigated opioid ligands, it represents a new opportunity to probe the pharmacology of the κOR by developing a new class of κOR agonists. To that end, this study, which represents the first comprehensive SAR investigation of **1**, provided several highly potent and selective κOR agonists.

By altering four different sites on the akuammicine scaffold, it became apparent that modifications to the C10 position uniquely led to increased κOR potency. Notably, analogues **2**-**6**, possessing halogens or aromatic substituents, possess similar levels of potency as some of the most potent κOR agonists discovered including U50,488, EOM salvinorin B, and triazole 1.1. It is noteworthy that the most potent of these compounds, **5**, bears a furan ring at C10, which is also found in the potent kappa agonists nalfurafine, triazole 1.1, and salvinorin A.[16,61,62] Recent cryo-EM studies revealed that the furan rings of nalfurafine and MOM-SalB, a derivative of salvinorin A, fill the same hydrophobic subpocket of the κOR binding site.[32,63] Similarly, dichlorobenzene in the arylacetamide GR89,696, and the iodobenzene in the morphan MP1104 also occupy this subpocket, indicating that this subpocket may be uniquely suited to bind furan rings and aryl halides.[63,64] Furthermore, the similar in potencies **2**, **3**, and **5** to these other κOR ligands suggests they may be making similar ligand-receptor interactions with this subpocket in order to enhance binding and potency at the κOR. Supporting this hypothesis, in the lowest energy conformation of **5** the furan ring and methyl ester are nearly perfectly aligned with those of MOM-SalB (**Figure S2**). Moreover, when this superimposed structure of **5** is placed in the κOR binding site, and further refined with Prime, the protonated amine of **5** is positioned in close proximity to Asp138 and forms salt-bridge interactions (**Figure 5**). Although additional studies are needed to validate this binding pose experimentally, it does appear to be consistent with the SAR trends described in this study.

Figure 5. Binding pose of **5** with the κOR predicted from alignment with MOM-SalB.

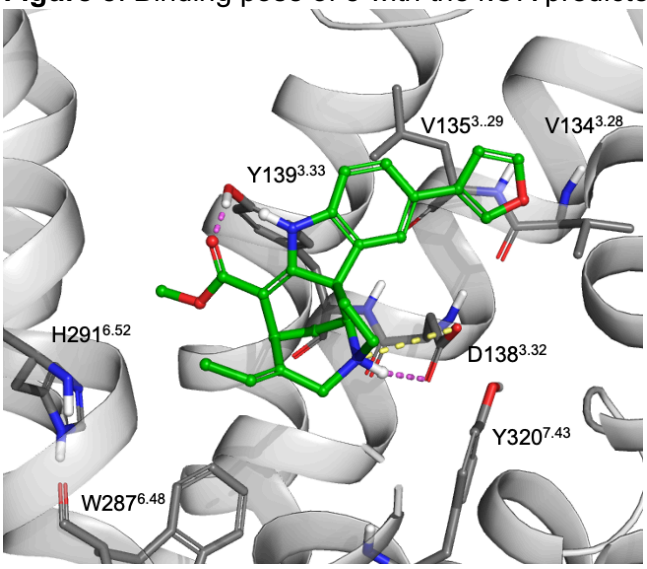

The structure of **5** was superimposed onto MOM-SalB bound to the κOR (PDB: 8DZP) by aligning their furan rings and esters. The **5**-κOR complex was further refined using Prime (Schrödinger Suite 2023-1). Salt-bridge interactions are shown in yellow. Hydrogen bond interactions shown in pink.

Additional *in vitro* screening demonstrated that the C10 halogenated analogues **2** and **3** display remarkable selectivity for the κOR in both binding and functional activity assays. Examining the effect of **2** and **3** for their ability to induce βArr2 recruitment, unmasked that these analogues potently recruit βArr2 indicating they are G-protein/βArr2 balanced agonists at the κOR. Driven in part by the early observations that the sedation and aversion may be βArr2-dependent, most recent κOR ligand development has focused on identifying G-protein biased agonists.[12,31,32,47,65,66] By comparison, few balanced κOR agonists have been discovered or investigated. However, not all G-protein biased κOR agonists are devoid of side effects. For example, RB64 produces significant CPA.[31] Instead, more nuanced events in the signaling cascade may be responsible for these adverse effects.[67,68] Given their potency and selectivity, **2, 3**, and other derivatives of **1** will be important tools to explore the behavioral effects of balanced κOR agonist and further refine the importance of βArr2-dependent signaling in κOR-mediated adverse effects.

Because the major adverse effects caused by κOR activation are centrally mediated, the development of peripherally restricted compounds has also been explored in pursuit of safer κOR agonists.[69] However, these efforts have generally been limited to peptides, which inherently can suffer from poor oral bioavailability and plasma stability.[70] With this in mind, we explored whether peripherally restricted agonists derived from **1** could be developed by alkylating its tertiary nitrogen. Because of the positive charge, these quaternary nitrogen cations are unlikely to transverse the blood-brain barrier. When applied to **1**, these modifications led to near complete loss in opioid activity (**16**-**20**). However, the bromination of C10 (**23**-**25**) was able to rescue much of this activity and resulted in compounds with moderate potency. Further exploration of the SAR may thus reveal other modifications that could lead to additional improvements in this activity and high potency, peripherally restricted κOR agonists. Furthermore, the only alkylated derivative of **1** that retained activity (**20**), and the most potent alkylated derivative of **2** (**25**), both contain a cyclopropylmethyl appendage. Notably, cycopropylmehtyl groups are also found on the nitrogen of several morphine-derived κOR ligands, including MP1104, BU74, and buprenorphine, with high κOR affinity.[71] This provides further support to our binding model depicted in **Figure 5** wherein the tertiary amine of **1** and its derivatives form similar interactions with the κOR as the morphinan nitrogen (i.e., salt-bridge interactions with Asp138$^{3.32}$).[64,72]

In conclusion, through a systematic investigation of the akuammicine scaffold this study has uncovered a new class of potent κOR ligands. Of note, halogenation and arylation of the C10 led to dramatic improvements in potency, suggesting the aryl ring of **1** is oriented to a subpocket of the κOR. These studies set the stage for future exploration of this complex natural product scaffold to probe how ligand-receptor interactions dictate downstream signaling events. Additionally, the halogenated derivatives, **2** and **3**, potently activate the κOR G-protein pathway and induce βArr2 recruitment indicating they are balanced agonists. As such, they offer new pharmacological tools to elucidate the mechanisms that govern the behavioral effects of κOR agonists.

Experimental

Chemistry

General Experimental Procedures. All solvents and reagents were purchased from commercial sources and used directly without further purification. Akuamma seed powder was purchased from Relax Remedy and alkaloids were isolated and purified as previously described. Bruker 400 MHz, Bruker 400 MHz HD, and Bruker 600 MHz spectrometers were used to record ^{1}H and ^{13}C NMR spectra, and they were referenced to the residual solvent peaks ($CHCl_3$:^{1}H δ= 7.26,^{13}C δ= 77.16 ppm). High-performance liquid chromatography (HPLC) was conducted on an Agilent 1260 Infinity II fitted with a DAD detector and PhenomenoxLuna Omega PS-C18 column (100×4.6 mm). A gradient of acetonitrile/water (20−45%) each containing 0.1% formic acid with a flow rate of 1 mL/min was used. The purity of all compounds was found to be >95% as determined by HPLC.

General procedure A: Akuammicine (**1**) (1.0 equiv) was placed in a clean, dry round-bottomed flask backfilled with nitrogen charged with a solution of 1:1 DCM/TFA (10 mL) on ice. NXS (1.1 eq) was dissolved in cooled 1:1 DCM/TFA (2 mL) and added dropwise to reaction mixture over 30 minutes while the reaction stirred at 0 °C. After the addition of NXS, the reaction was allowed to stir at 0 °C for 3 h. Upon consumption of the starting material as indicated by TLC (9:1 DCM:MeOH), the reaction mixture was basified to pH 9-10 with 28% NH_4OH (aq). The aqueous layer was extracted with DCM (3 x 10 mL). The combined organic layers were dried with Na_2SO_4, filtered, and concentrated in vacuo. The crude residue was purified via silica gel chromatography (0-6% MeOH/DCM) to afford the product as an off-white solid.

General procedure B: To a clean, oven dried sealed tube was added $Pd(PPh_3)_4$ (0.05 equiv), $RB(OH)_2$ (2.0 equiv), oven dried K_2CO_3 (2.0 equiv), and **3** (1.0 equiv). The tube was sealed and purged with nitrogen. 2 mL of anhydrous toluene and anhydrous methanol (3:2) were degassed and injected into the tube. The reaction was heated to 80 °C for 24 h followed by cooling to room

temperature and removal of solvent in vacuo. The crude residue was purified via silica gel chromatography (0-5% MeOH/DCM) to afford the product as a white solid.

General Procedure C: To a clean, oven-dried round bottom flask **1** or **2** (1 equiv) and NMO (3 equiv) was dissolved in a 3:2:1 solution of THF/tBuOH/H_2O (15 mL). The flask was purged with nitrogen and a catalytic amount of OsO_4 (4% wt. in H_2O, 0.1 mL) was added via syringe. The reaction was stirred for 12-18 h. The reaction was quenched with $Na_2S_2O_3$(40% w.t. in H_2O) and extracted with DCM (4 x 30 mL). The combined organic layers were dried with Na_2SO_4, filtered, and concentrated under vacuum. The residue was purified using silica gel chromatography (6-10% MeOH in DCM, 5% NH_4OH by vol.) to give the final products as white solids.

General Procedure D: 1, **2**, or **3** (1.0 equiv) were placed into a clean, dry round bottom flask and backfilled with nitrogen. The flask was charged with a 3:2 solution of AcOH/H_2O (5 mL) on ice. To the cooled solution was added $NaCNBH_3$ (1.1 equiv) and the reaction was stirred for 4 h. The reaction was diluted with DCM and basified with 28% NH_4OH (aq). The aqueous layer was extracted with DCM (4 x 10 mL). The combined organic layers were dried with Na_2SO_4, filtered, and concentrated in vacuo. The residue was purified using silica gel chromatography (0-4% MeOH in DCM) to give the final products as white solids.

General Procedure E: 1 or **2** (1.0 equiv) was placed in a clean, dry round-bottomed flask backfilled with nitrogen and dissolved in anhydrous chloroform (5 mL). Alkyl halide RI or RBr (200 equiv) was added to the flask via syringe at room temperature. The reaction was heated to 60 °C until consumption of the starting material as indicated by TLC (9:1 DCM:MeOH). The reaction mixture was cooled to room temperature and concentrated *in vacuo*. The residue was chromatographed over silica gel pre-treated with 12% NaBr in MeOH (4-10% MeOH in DCM) to yield the final products as white solids.

*10-Bromoakuammicine (**2**).* Prepared from **1** according to General Procedure A to yield 161 mg (86%) of **2**. ^{1}H NMR (400 MHz, $CDCl_3$) δ 8.98 (s, 1H), 7.37 (d, J = 2.0 Hz, 1H), 7.28 (dd, J = 8.3, 2.0 Hz, 1H), 6.71 (d, J = 8.3 Hz, 1H), 5.47 (q, J = 7.3 Hz, 1H), 4.21 (s, 1H), 4.02 (d, J = 18.6 Hz, 2H), 3.81 (s, 3H), 3.46 – 3.40 (m, 1H), 3.16 – 3.04 (m, 2H), 2.57 (td, J = 12.9, 6.9 Hz, 1H), 2.50 – 2.43 (m, 1H), 1.96 (dd, J = 12.8, 5.9 Hz, 1H), 1.63 (dt, J = 7.0, 1.8 Hz, 3H), 1.35 (dt, J = 13.8, 2.9 Hz, 1H). ^{13}C NMR (101 MHz, $CDCl_3$) δ 167.97, 166.99, 142.67, 139.02, 138.42, 130.70, 124.28, 121.39, 113.24, 110.91, 102.14, 62.00, 57.62, 56.76, 56.15, 51.28, 46.18, 30.90, 29.76, 13.02. HRMS calculated for $C_{20}H_{22}N_2O_2Br$: $[M + H]^+$: 401.0868 (found); 401.0865 (calcd).

*10-Iodoakuammicine (**3**).* Prepared from **1** according to General Procedure A to yield 167 mg (80%) of **3**. ^{1}H NMR (400 MHz, $CDCl_3$) δ 8.98 (s, 1H), 7.52 (s, 1H), 7.46 (d, J = 8.2 Hz, 1H), 6.61 (d, J = 8.2 Hz, 1H), 5.43 (q, 1H), 4.13 (s, 1H), 3.97 (s, 2H), 3.81 (d, J = 1.0 Hz, 3H), 3.36 (s, 1H), 3.13 – 3.00 (m, 2H), 2.55 (td, J = 12.9, 6.8 Hz, 1H), 2.44 (d, J = 13.8 Hz, 1H), 1.92 (s, 1H), 1.62 (d, J = 6.9 Hz, 3H), 1.33 (d, J = 13.6 Hz, 1H). ^{13}C NMR (101 MHz, $CDCl_3$) δ 167.86, 166.30, 143.30, 139.05, 137.58, 136.89, 129.88, 122.24, 111.65, 102.23, 82.91, 62.02, 57.21, 56.65, 55.99, 51.33, 45.85, 30.71, 29.63, 13.09. HRMS calculated for $C_{20}H_{22}N_2O_2I$: $[M + H]^+$: 449.0727 (found); 449.0726 (calcd).

*10-Phenylakuammicine (**4**).* Prepared from **3** (15 mg, 0.033 mmol) according to General Procedure B to yield 13 mg (73%) of **4**. ^{1}H NMR (400 MHz, $CDCl_3$) δ 9.04 (s, 1H), 7.56 – 7.47 (m, 3H), 7.46 – 7.37 (m, 3H), 7.30 (t, J = 7.6 Hz, 1H), 6.91 (d, J = 8.2 Hz, 1H), 5.51 (q, J = 7.2 Hz, 1H), 4.39 (s, 1H), 4.10 (d, J = 14.9 Hz, 1H), 4.03 (s, 1H), 3.83 (s, 3H), 3.55 (td, J = 12.6, 6.0 Hz, 1H), 3.21 – 3.11 (m, 2H), 2.62 (td, J = 13.0, 6.8 Hz, 1H), 2.57 – 2.44 (m, 1H), 2.04 (dd, J = 12.8, 5.3 Hz, 1H), 1.66 (d, J = 7.0 Hz, 3H), 1.42 (dt, J = 13.7, 2.9 Hz, 1H). ^{13}C NMR (101 MHz, $CDCl_3$) δ 167.91, 167.16, 142.91, 141.11, 137.55, 137.08, 134.84, 128.97, 127.19, 126.98, 126.89,

122.61, 119.89, 109.88, 101.90, 62.05, 57.24, 56.71, 55.97, 51.29, 45.82, 30.74, 29.66, 13.16. HRMS calculated for $C_{26}H_{27}N_2O_2$: $[M + H]^+$: 399.2074 (found); 399.2073 (calcd).

*10-(3-Furanyl)akuammicine (**5**).* Prepared from **3** (40 mg, 0.0892 mmol) according to General Procedure B to yield 15.3 mg (44%) of **5**. ^{1}H NMR (600 MHz, $CDCl_3$) δ 9.00 (s, 1H), 7.68 (t, J = 1.2 Hz, 1H), 7.45 (t, J = 1.7 Hz, 1H), 7.41 (d, J = 1.6 Hz, 1H), 7.31 (dd, J = 8.0, 1.7 Hz, 1H), 6.84 (d, J = 8.1 Hz, 1H), 6.65 (dd, J = 1.9, 0.9 Hz, 1H), 5.49 (q, J = 7.3 Hz, 1H), 4.35 (s, 1H), 4.06 (d, J = 14.9 Hz, 1H), 4.01 (s, 1H), 3.82 (s, 3H), 3.54 (s, 1H), 3.13 (m, J = 6.4 Hz, 2H), 2.59 (td, J = 12.9, 6.8 Hz, 1H), 2.48 (ddd, J = 13.9, 4.1, 2.3 Hz, 1H), 2.01 (dd, J = 12.8, 5.9 Hz, 1H), 1.65 (dt, J = 7.0, 1.8 Hz, 3H), 1.39 (dt, J = 14.0, 3.0 Hz, 1H), 0.88 (td, J = 6.9, 1.8 Hz, 1H). ^{13}C NMR (151 MHz, $CDCl_3$) δ 167.74, 166.43, 143.85, 142.38, 137.97, 136.48, 136.24, 126.31, 126.12, 126.05, 124.05, 118.84, 110.04, 108.92, 101.86, 61.91, 56.51, 55.69, 51.36, 45.24, 30.43, 29.84, 29.41, 13.28. HRMS calculated for $C_{24}H_{25}N_2O_3$: $[M + H]^+$: 389.1858 (found); 389.1865 (calcd).

*10-(3-Thienyl)akuammicine (**6**).* Prepared from **3** (40 mg, 0.0892 mmol) according to General Procedure B to yield 16.0 mg (44%) of **6**. ^{1}H NMR (600 MHz, $CDCl_3$) δ 9.02 (s, 1H), 7.54 (s, 1H), 7.41 (dd, J = 8.1, 1.6 Hz, 1H), 7.37 – 7.32 (m, 3H), 6.85 (d, J = 8.1 Hz, 1H), 5.46 (d, J = 7.4 Hz, 1H), 4.31 (s, 1H), 4.03 (d, J = 15.4 Hz, 1H), 3.99 (s, 1H), 3.82 (s, 3H), 3.51 (s, 1H), 3.13 (d, J = 9.1 Hz, 1H), 3.11 (s, 1H), 2.58 (td, J = 12.8, 6.7 Hz, 1H), 2.50 – 2.46 (m, 1H), 1.98 (dd, J = 12.8, 5.8 Hz, 1H), 1.64 (dt, J = 7.0, 1.7 Hz, 3H), 1.37 (d, J = 13.8 Hz, 1H). ^{13}C NMR (151 MHz, $CDCl_3$) δ 167.80, 166.71, 142.52, 142.15, 136.74, 135.87, 129.73, 126.57, 126.43, 126.30, 123.41, 119.40, 119.30, 109.89, 101.90, 61.85, 56.93, 56.49, 55.72, 51.33, 45.50, 30.54, 29.50, 13.23. HRMS calculated for $C_{24}H_{25}N_2O_3S$: $[M + H]^+$: 405.1631 (found); 405.1637 (calcd).

*10-Cyanoakuammicine (**7**).* An oven dried, Schlenk tube was charged with **2** (30 mg, 0.075 mmol), Pd G3 tBuXPhos (3.6 mg, 0.004 mmol, 0.06 eq), and $Zn(CN)_2$ (6.6 mg, 0.056 mmol, 0.75 eq) and placed under an atmosphere of nitrogen. 2 mL of 1,4-dioxane and H_2O were added to the tube and the reaction was heated to 85°C for 24 h. The reaction was cooled to room temperature and quenched with saturated $NaHCO_3$ (aq) and EtOAc, then stirred for 10 minutes. The reaction mixture was extracted with EtOAc (3 x 5 ml). The combined organic layers were dried with Na_2SO_4, filtered, and concentrated under vacuum. The crude residue was purified via silica gel chromatography (2-5% MeOH/DCM) to afford the product as an off-white solid (7.6 mg, 29% yield). ^{1}H NMR (400 MHz, $CDCl_3$) δ 9.22 (s, 1H), 7.51 – 7.44 (m, 2H), 6.85 (d, J = 8.1 Hz, 1H), 5.41 (q, J = 6.7 Hz, 1H), 4.09 (s, 1H), 3.99 – 3.88 (m, 2H), 3.82 (s, 3H), 3.37 – 3.25 (m, 1H), 3.08 (dd, J = 12.6, 6.2 Hz, 1H), 3.00 (d, J = 15.0 Hz, 1H), 2.53 (td, J = 12.7, 6.8 Hz, 1H), 2.45 (ddd, J = 13.7, 4.0, 2.3 Hz, 1H), 1.86 (dd, J = 12.7, 5.0 Hz, 1H), 1.60 (dt, J = 6.8, 1.8 Hz, 3H), 1.32 (dt, J = 13.7, 3.2 Hz, 1H).^{13}C NMR (101 MHz, $CDCl_3$) δ 167.76, 165.45, 147.30, 138.04, 137.73, 133.49, 124.49, 121.70, 119.78, 109.74, 104.25, 103.61, 62.11, 57.05, 56.72, 56.24, 51.50, 46.37, 30.80, 29.83, 13.04. HRMS calculated for $C_{21}H_{22}N_3O_2$: $[M + H]^+$: 348.1710 (found); 348.1712 (calcd).

*10-Nitroakuammicine (**8**).* In an oven-dried round bottomed flask, **1** (40 mg, 0.12 mmol) was dissolved in anhydrous DCM. To the solution was added concentrated HNO_3 (420 mg, 6.7 mmol, 55 equiv). The reaction was allowed to stir for 1 h, then set in a cooling bath. The reaction was diluted with DI H_2O and saturated $NaHCO_3$ (aq) was added dropwise until basic. The aqueous solution was extracted with DCM (5 x 10 mL). The combined organic layers were dried with Na_2SO_4, filtered, and concentrated under vacuum. The crude sample was purified via silica gel chromatography (0-4% MeOH/DCM) to afford the product as a bright yellow solid (30 mg, 64% yield). ^{1}H NMR (400 MHz, $CDCl_3$) δ 9.36 (s, 1H), 8.16 (dd, J = 8.6, 2.3 Hz, 1H), 8.11 (d, J = 2.3 Hz, 1H), 6.86 (d, J = 8.7 Hz, 1H), 5.40 (q, J = 7.0 Hz, 1H), 4.11 – 4.05 (m, 1H), 3.98 (s, 1H), 3.92

– 3.82 (m, 4H), 3.31 (td, J = 12.6, 5.7 Hz, 1H), 3.08 (dd, J = 12.6, 6.6 Hz, 1H), 2.98 (d, J = 15.1 Hz, 1H), 2.56 (td, J = 12.6, 6.8 Hz, 1H), 2.46 (ddd, J = 13.5, 4.0, 2.3 Hz, 1H), 1.87 (dd, J = 12.5, 5.6 Hz, 1H), 1.62 (dt, J = 6.9, 1.7 Hz, 3H), 1.34 (dt, J = 13.6, 3.0 Hz, 1H). ^{13}C NMR (101 MHz, $CDCl_3$) δ 167.74, 165.77, 149.19, 141.93, 138.36, 137.75, 125.75, 121.15, 117.14, 108.55, 105.20, 62.32, 57.17, 56.83, 56.43, 51.55, 46.57, 30.95, 30.00, 12.99. HRMS calculated for $C_{20}H_{22}N_3O_4$: $[M + H]^+$: 368.1612 (found); 368.1610 (calcd).

*10-Aminoakuammicine (**9**).* In an oven-dried round bottom flask, **13** (35 mg, 0.095 mmol) and $SnCl_2$ (91 mg, 0.48 mmol, 5 eq) were dissolved in anhydrous EtOH. The flask was purged with nitrogen and heated to 70 °C for 4 h. The reaction was cooled to room temperature and concentrated under vacuum. The resulting residue was purified using silica gel chromatography (10-20% MeOH in DCM with 5% NH_4OH by vol.). The final product was obtained as a tan solid (17 mg, 52% yield). ^{1}H NMR (400 MHz, $CDCl_3$) δ 8.84 (s, 1H), 6.68 (d, J = 2.2 Hz, 1H), 6.63 (d, J = 8.1 Hz, 1H), 6.50 (dd, J = 8.2, 2.2 Hz, 1H), 5.38 (q, J = 7.1 Hz, 1H), 4.06 (s, 1H), 3.97 – 3.89 (m, 2H), 3.79 (s, 3H), 3.32 (ddd, J = 12.6, 12.6, 5.8 Hz, 1H), 3.08 – 2.95 (m, 2H), 2.52 (ddd, J = 12.7, 12.7, 6.8 Hz, 1H), 2.42 (ddd, J = 13.6, 4.0, 2.3 Hz, 1H), 1.87 (dd, J = 12.5, 5.7 Hz, 1H), 1.61 (dt, J = 7.0, 1.7 Hz, 3H), 1.31 (dt, J = 13.4, 3.0 Hz, 1H).^{13}C NMR (101 MHz, $CDCl_3$) δ 168.53, 168.13, 140.89, 139.27, 138.44, 136.04, 120.90, 114.18, 110.08, 109.38, 100.12, 62.07, 57.98, 57.07, 56.33, 51.01, 46.27, 31.12, 29.84, 13.00. HRMS calculated for $C_{20}H_{24}N_3O_2$: $[M + H]^+$: 338.1869 (found); 338.1869 (calcd).

*19R,20R-Dihydroxyakuammicine (**10**)* and *19S,20S-Dihydroxyakuammicine (**11**).* Prepared from **1** (300 mg, 0.93 mmol) according to General Procedure C to afford 246 mg (74%) of **10** and 30.5 mg (9%) of **11**. The ^{1}H and ^{13}C NMR spectra of **10** were consistent with previously published spectral data.[40] Compound **11:** ^{1}H NMR (400 MHz, $CDCl_3$) δ 8.71 (s, 1H), 7.21 – 7.12 (m, 2H), 6.93 (t, J = 7.4 Hz, 1H), 6.85 (d, J = 7.8 Hz, 1H), 4.00 (q, J = 6.4 Hz, 1H), 3.93 (s, 1H), 3.84 (s,

3H), 3.28 (d, J = 12.3 Hz, 1H), 3.18 – 3.11 (m, 1H), 3.09 (d, J = 4.1 Hz, 2H), 3.01 – 2.83 (m, 2H), 2.33 (d, J = 12.3 Hz, 1H), 2.02 (dt, J = 13.7, 3.3 Hz, 1H), 1.87 (ddd, J = 13.0, 6.7, 1.9 Hz, 1H), 1.28 (d, J = 6.4 Hz, 3H). ^{13}C NMR (101 MHz, $CDCl_3$) δ 171.70, 169.26, 144.05, 135.48, 127.93, 121.62, 120.33, 109.94, 97.84, 72.80, 69.84, 59.77, 58.01, 54.30, 52.64, 51.84, 44.18, 35.65, 27.19, 16.82. HRMS calculated for $C_{20}H_{25}N_2O_4$: $[M + H]^+$: 357.1808 (found); 357.1814 (calcd).

*19-Hydroxyalstolucine (**12**).* In a round bottomed flask, **10** (19.8 mg, 0.056 mmol, 1 eq) was dissolved in DCM. Dess-Martin periodinane (47.5 mg, 0.122 mmol, 2 eq) and a drop of water were added. The flask was placed under nitrogen and allowed to stir at room temperature for 3-5 h. The reaction was quenched with saturated $NaHCO_3$(aq) and 40% wt. $Na_2S_2O_3$ (aq) in a 1:1 ratio. The aqueous layer was extracted with DCM. The combined organic layers were washed with brine, dried with Na_2SO_4, filtered, and concentrated under vacuum. The residue was purified using silica gel chromatography (0-5% MeOH in DCM) to give the product as an off-white solid (10.2 mg, 54% yield). The ^{1}H NMR was consistent with previously published spectral data.[40,73]

*19,20-dihydroakuammicine (**13**).* An oven-dried, round bottom flask was charged with **1** (50 mg, 0.19 mmol) and PtO_2 (6 mg, 10% by wt.) was added MeOH. The reaction was placed under an atmosphere of H_2 (g) and stirred for 8 h. Upon completion according to consumption of starting material by TLC, the reaction mixture was filtered through Celite and concentrated under vacuum. The residue was purified via silica gel flash chromatography (3-5% MeOH in DCM) to afford the final product as a white solid (53.2 mg, 88% yield). ^{1}H NMR (400 MHz, $CDCl_3$) δ 9.04 (s, 1H), 7.21 (d, J = 7.4 Hz, 1H), 7.17 (td, J = 7.7, 1.1 Hz, 1H), 6.93 (t, J = 7.5 Hz, 1H), 6.84 (d, J = 7.8 Hz, 1H), 4.21 (s, 1H), 3.77 (s, 3H), 3.43 – 3.12 (m, 3H), 3.08 – 2.84 (m, 2H), 2.32 – 2.12 (m, 2H), 2.01 (dd, J = 13.1, 7.3 Hz, 1H), 1.95 – 1.82 (m, 1H), 1.48 (ddd, J = 13.5, 4.0, 2.5 Hz, 1H), 1.40 (dt, J = 13.3, 7.0 Hz, 1H), 1.14 – 0.97 (m, 4H). ^{13}C NMR (101 MHz, $CDCl_3$) δ 170.16, 168.59, 144.37, 133.96, 128.38, 121.58, 119.90, 110.12, 98.76, 61.12, 55.20, 53.24, 51.34, 50.84, 41.58, 38.53, 30.69,

30.11, 25.89, 11.57. HRMS calculated for $C_{20}H_{25}N_2O_2$: $[M + H]^+$: 325.1916 (found); 325.1916 (calcd).

*2,16-dihydroakuammicine (**14**).* Prepared from **1** (40 mg, 0.0892 mmol) according to General Procedure D to yield 78 mg (97%) of **15** without further purification. ^{1}H NMR (400 MHz, $CDCl_3$) δ 7.12 – 7.00 (m, 2H), 6.78 (td, J = 7.4, 1.0 Hz, 1H), 6.61 (d, J = 7.7 Hz, 1H), 5.29 (q, J = 6.6 Hz, 1H), 4.15 (t, J = 4.7 Hz, 1H), 4.07 (d, J = 4.3 Hz, 1H), 3.79 (s, 3H), 3.60 – 3.52 (m, 2H), 3.24 – 3.20 (m, 1H), 3.20 – 3.10 (m, 2H), 2.96 (dt, J = 10.8, 6.8 Hz, 1H), 2.70 (dd, J = 5.4, 3.1 Hz, 1H), 2.41 (dt, J = 13.5, 7.2 Hz, 1H), 2.22 (ddd, J = 13.9, 3.9, 1.8 Hz, 1H), 2.10 (dt, J = 12.9, 6.3 Hz, 1H), 1.71 (ddd, J = 13.8, 4.5, 2.9 Hz, 1H), 1.62 (dd, J = 6.9, 1.4 Hz, 3H). ^{13}C NMR (101 MHz, $CDCl_3$) δ 174.72, 149.66, 140.87, 135.24, 128.02, 122.62, 119.75, 118.60, 110.02, 65.07, 64.35, 54.24, 54.04, 52.51, 52.33, 46.77, 38.59, 27.19, 23.17, 12.75. HRMS calculated for $C_{20}H_{25}N_2O_2$: $[M + H]^+$: 325.1913 (found); 325.1916 (calcd).

*2,16,19,20-tetrahydroakuammicine (**15**).* To a round bottom flask with a 1:1 solution of AcOH/DI H_2O (2.5 mL) cooled to 0 °C was added was **7** (18 mg, 0.056 mmol) and $NaCNBH_3$ (18 mg, 0.29 mmol, 5 eq). The reaction flask was purged with nitrogen and the reaction was stirred for 3 h. The reaction was diluted with $CHCl_3$ and basified with 28% NH_4OH (aq). The aqueous layer was extracted with $CHCl_3$ (4 x 5 ml). The combined organic layers were dried with Na_2SO_4, filtered, and concentrated under vacuum. (15 mg, 82% yield). ^{1}H NMR (400 MHz, $CDCl_3$) δ 7.10 – 6.98 (m, 2H), 6.77 (t, J = 7.4 Hz, 1H), 6.59 (d, J = 7.7 Hz, 1H), 4.20 (d, J = 3.4 Hz, 2H), 3.78 (s, 3H), 3.16 – 3.03 (m, 1H), 3.02 – 2.84 (m, 3H), 2.60 (dt, J = 19.6, 3.3 Hz, 2H), 2.35 – 2.15 (m, 4H), 1.74 – 1.64 (m, 2H), 1.32 – 1.20 (m, 1H), 1.17 – 1.06 (m, 1H), 0.95 (t, J = 7.3 Hz, 3H).^{13}C NMR (101 MHz, $CDCl_3$) δ 175.24, 149.26, 137.31, 127.80, 122.35, 119.77, 109.78, 67.05, 64.70, 55.63, 54.02, 52.30, 50.32, 42.67, 39.60, 39.00, 27.46, 26.15, 24.44, 11.67. HRMS calculated for $C_{20}H_{27}N_2O_2$: $[M + H]^+$: 327.2075 (found); 327.2073 (calcd).

*N-4-Methylakuammicine (**16**).* Prepared from **1** according to General Procedure E using methyl iodide (200 equiv) to afford 18 mg (65%) of **16**. ^{1}H NMR (400 MHz, $CDCl_3$) δ 8.82 (s, 1H), 8.03 (d, J = 7.5 Hz, 1H), 7.20 (t, J = 7.7 Hz, 1H), 7.01 (t, J = 7.5 Hz, 1H), 6.84 (d, J = 7.8 Hz, 1H), 5.86 (q, J = 6.8 Hz, 1H), 4.90 (s, 1H), 4.54 – 4.32 (m, 3H), 4.23 – 4.10 (m, 2H), 3.89 (s, 3H), 3.80 (s, 3H), 2.97 – 2.84 (m, 1H), 2.52 (dt, J = 14.9, 3.2 Hz, 1H), 2.25 (dd, J = 14.2, 7.2 Hz, 1H), 1.78 (d, J = 7.0 Hz, 3H), 1.68 – 1.57 (m, 1H). ^{13}C NMR (101 MHz, $CDCl_3$) δ 166.95, 165.38, 143.24, 132.31, 129.43, 129.24, 128.16, 122.71, 122.65, 110.32, 101.43, 77.48, 77.16, 76.84, 72.82, 64.73, 63.35, 55.26, 51.75, 50.81, 40.92, 29.83, 28.28, 28.10, 13.40. HRMS calculated for $C_{21}H_{25}N_2O_2$: $[M + H]^+$: 337.1922 (found); 337.1916 (calcd).

*N-4-Allylakuammicine (**17**).* Prepared from **1** according to General Procedure E using allyl bromide (200 equiv) to afford 17 mg (83%) of **17**. ^{1}H NMR (400 MHz, $CDCl_3$) δ 8.84 (s, 1H), 7.96 (d, *J* = 7.5 Hz, 1H), 7.19 (m, 1H), 7.00 (td, *J* = 7.6, 1.1 Hz, 1H), 6.84 (d, *J* = 7.8 Hz, 1H), 6.21 (ddt, *J* = 17.0, 9.7, 7.3 Hz, 1H), 6.00 (d, *J* = 16.9 Hz, 1H), 5.80 (m, 2H), 5.16 (dd, *J* = 12.8, 6.8 Hz, 1H), 5.05 (d, *J* = 3.1 Hz, 1H), 4.50 (m, 2H), 4.21 (s, 1H), 4.14 (s, 1H), 3.94 (dd, *J* = 11.9, 7.2 Hz, 1H), 3.81 (s, 3H), 2.87 (td, *J* = 13.7, 7.3 Hz, 1H), 2.65 (dt, *J* = 14.8, 3.2 Hz, 1H), 2.23 (dd, *J* = 14.2, 7.3 Hz, 1H), 1.76 (d, *J* = 7.0 Hz, 4H), 1.61 (s, 1H).^{13}C NMR (101 MHz, $CDCl_3$) δ 166.97, 165.07, 143.08, 132.63, 130.47, 129.42, 129.29, 129.07, 125.39, 122.65, 122.59, 110.29, 101.53, 71.04, 63.58, 61.80, 60.36, 55.20, 51.72, 40.89, 28.72, 28.33, 13.51. HRMS calculated for $C_{23}H_{27}N_2O_2$: $[M + H]^+$: 363.2068 (found); 363.2073 (calcd).

*N-4-Propylakuammicine (**18**).* Prepared from **1** according to General Procedure E using 1-bromopropane (200 equiv) to afford 20 mg (90%) of **18**. ^{1}H NMR (400 MHz, $CDCl_3$) δ 8.85 (s, 1H), 7.93 (d, J = 7.5 Hz, 1H), 7.19 (d, J = 7.6 Hz, 1H), 6.98 (t, J = 7.5 Hz, 1H), 6.84 (d, J = 7.8 Hz, 1H), 5.89 (q, J = 6.9 Hz, 1H), 4.86 – 4.74 (m, 1H), 4.42 (d, J = 14.2 Hz, 1H), 4.39 – 4.28 (m, 1H), 4.28

– 4.15 (m, 3H), 4.12 (s, 1H), 3.90 (td, J = 12.0, 5.3 Hz, 1H), 3.80 (s, 3H), 2.89 (td, J = 13.8, 7.3 Hz, 1H), 2.73 (dt, J = 14.9, 3.2 Hz, 1H), 2.18 (dt, J = 12.4, 6.2 Hz, 1H), 2.11 – 1.95 (m, 2H), 1.71 (d, J = 6.9 Hz, 3H), 1.56 (d, J = 14.9 Hz, 1H), 1.12 (t, J = 7.2 Hz, 3H). ^{13}C NMR (101 MHz, $CDCl_3$) δ 166.95, 164.47, 142.97, 132.87, 129.72, 129.65, 129.41, 122.52, 122.39, 110.28, 101.68, 77.48, 77.16, 76.84, 73.36, 65.03, 62.19, 61.11, 55.12, 51.66, 41.61, 28.85, 28.47, 17.72, 13.57, 11.05. HRMS calculated for $C_{23}H_{29}N_2O_2$: $[M + H]^+$: 365.2223 (found); 365.2229 (calcd).

*N-4-Cyclopropylmethylakuammicine (**19**).* Prepared from **1** according to General Procedure E using bromomethyl cyclopropyl (200 equiv) to afford 17 mg (77%) of **19**. ^{1}H NMR (400 MHz, $CDCl_3$) δ 8.84 (s, 1H), 7.98 (d, J = 7.5 Hz, 1H), 7.19 (t, J = 7.7 Hz, 1H), 6.99 (t, J = 7.5 Hz, 1H), 6.84 (d, J = 7.8 Hz, 1H), 5.83 (q, J = 6.9 Hz, 1H), 5.01 (d, J = 3.2 Hz, 1H), 4.50 (td, J = 12.6, 7.4 Hz, 1H), 4.40 – 4.28 (m, 3H), 4.21 – 4.09 (m, 2H), 3.89 (dd, J = 13.2, 6.9 Hz, 1H), 3.80 (s, 3H), 2.91 (td, J = 13.7, 7.2 Hz, 1H), 2.62 (dt, J = 14.8, 3.2 Hz, 1H), 2.24 (dd, J = 14.2, 7.2 Hz, 1H), 1.75 (d, J = 7.0 Hz, 3H), 1.57 (dt, J = 14.8, 2.9 Hz, 1H), 1.32 – 1.20 (m, 2H), 0.91 – 0.82 (m, 3H).^{13}C NMR (101 MHz, $CDCl_3$) δ 166.97, 165.07, 143.08, 132.76, 129.38, 129.27, 129.15, 122.59, 122.53, 110.27, 101.53, 71.39, 65.91, 61.65, 60.67, 55.16, 51.69, 41.19, 28.74, 28.38, 13.49, 5.87, 5.20, 5.05. HRMS calculated for $C_{24}H_{29}N_2O_2$: $[M + H]^+$: 377.2231 (found); 377.2229 (calcd).

*N-4-Benzylakuammicine (**20**).* Prepared from **1** according to General Procedure E using benzyl bromide (200 equiv) to afford 21 mg (86%) of **20**. ^{1}H NMR (400 MHz, $CDCl_3$) δ 8.81 (s, 1H), 7.88 – 7.81 (m, 2H), 7.53 – 7.42 (m, 3H), 7.24 (d, J = 7.5 Hz, 1H), 7.14 (td, J = 7.8, 1.1 Hz, 1H), 6.88 – 6.77 (m, 2H), 5.82 – 5.73 (m, 2H), 5.20 (d, J = 12.6 Hz, 1H), 5.09 (d, J = 3.2 Hz, 1H), 4.49 (td, J = 12.5, 7.3 Hz, 1H), 4.34 (d, J = 14.3 Hz, 1H), 4.26 (d, J = 14.3 Hz, 1H), 4.16 (s, 1H), 3.89 (dd, J = 11.8, 7.0 Hz, 1H), 3.80 (s, 3H), 2.91 – 2.71 (m, 2H), 2.15 – 2.05 (m, 1H), 1.75 (d, J = 7.4 Hz, 3H), 1.58 (dd, J = 11.0, 7.3 Hz, 1H). ^{13}C NMR (101 MHz, $CDCl_3$) δ 166.99, 164.90, 142.96, 133.94, 132.80, 130.82, 129.69, 129.46, 129.26, 129.21, 128.14, 122.45, 122.18, 110.18, 101.62, 77.48,

77.16, 76.84, 69.63, 63.74, 62.08, 59.45, 55.04, 51.66, 40.73, 31.69, 29.81, 28.55, 28.45, 22.76, 14.22, 13.54. HRMS calculated for $C_{27}H_{29}N_2O_2$: $[M + H]^+$: 413.2233 (found); 413.2229 (calcd).

*10-Bromo-2,16-dihydroakuammicine (**21**).* Prepared from **2** (28.3 mg, 0.0705 mmol) according to General Procedure D to yield 13.0 mg of **21** (46%). ^{1}H NMR (600 MHz, $CDCl_3$) δ 7.15 (d, J = 2.0 Hz, 1H), 7.13 (dd, J = 8.2, 2.0 Hz, 1H), 6.48 (d, J = 8.2 Hz, 1H), 5.34 (q, J = 7.6 Hz, 1H), 4.16 – 4.11 (m, 2H), 3.77 (s, 3H), 3.58 (d, J = 14.7 Hz, 1H), 3.53 (t, J = 3.4 Hz, 1H), 3.28 – 3.25 (m, 1H), 3.24 – 3.15 (m, 2H), 2.96 (dt, J = 11.1, 6.9 Hz, 1H), 2.71 (dd, J = 5.3, 3.1 Hz, 1H), 2.36 (dt, J = 14.1, 7.3 Hz, 1H), 2.22 (ddd, J = 14.0, 3.9, 1.9 Hz, 1H), 2.11 (dt, J = 13.1, 6.3 Hz, 1H), 1.77 – 1.71 (m, 1H), 1.67 – 1.60 (m, 3H). ^{13}C NMR (151 MHz, $CDCl_3$) δ 174.29, 148.61, 139.28, 137.08, 130.87, 125.75, 119.82, 111.40, 111.24, 64.74, 64.22, 54.20, 53.76, 52.45, 52.34, 46.40, 38.33, 27.11, 22.92, 12.84. HRMS calculated for $C_{20}H_{22}N_2O_2Br$: $[M + H]^+$: 403.1019 (found); 403.1016 (calcd).

*10-Iodo-2,16-dihydroakuammicine (**22**).* Prepared from **3** (30.0 mg, 0.0669 mmol) according to General Procedure D to yield 11.3 mg of **22** (36%). ^{1}H NMR (600 MHz, $CDCl_3$) δ 7.34 – 7.29 (m, 2H), 6.40 (d, J = 8.1 Hz, 1H), 5.35 (q, J = 7.6 Hz, 1H), 4.16 – 4.11 (m, 2H), 3.77 (s, 3H), 3.60 (d, J = 14.7 Hz, 1H), 3.53 (q, J = 3.3 Hz, 1H), 3.30 – 3.26 (m, 1H), 3.25 – 3.21 (m, 1H), 3.20 – 3.15 (m, 1H), 2.96 (dt, J = 11.1, 6.9 Hz, 1H), 2.71 (dd, J = 5.4, 3.1 Hz, 1H), 2.35 (dt, J = 14.2, 7.3 Hz, 1H), 2.22 (ddd, J = 14.1, 3.9, 1.9 Hz, 1H), 2.11 (dt, J = 13.1, 6.3 Hz, 1H), 1.75 (ddd, J = 14.0, 4.5, 3.0 Hz, 1H), 1.63 (dt, J = 6.9, 1.4 Hz, 3H). ^{13}C NMR (151 MHz, $CDCl_3$) δ 174.23, 149.27, 138.97, 137.41, 136.87, 131.49, 120.09, 112.10, 80.43, 64.67, 64.02, 54.04, 53.70, 52.47, 52.30, 46.37, 38.27, 27.09, 22.85, 12.86. HRMS calculated for $C_{20}H_{24}N_2O_2I$: $[M + H]^+$: 451.0887 (found); 451.0882 (calcd).

*10-Bromo-N-4-methylakuammicine (**23**).* Prepared from **2** (20.3 mg, 0.05059 mmol) according to General Procedure E using methyl iodide (200 equiv) to yield 29 mg of **23** (quant). ^{1}H NMR (600 MHz, $CDCl_3$) δ 8.83 (s, 1H), 8.31 (d, J = 1.9 Hz, 1H), 7.29 (dd, J = 8.3, 1.9 Hz, 1H), 6.73 (d, J = 8.3 Hz, 1H), 5.87 – 5.81 (m, 1H), 5.04 (d, J = 3.2 Hz, 1H), 4.51 (td, J = 12.3, 7.4 Hz, 1H), 4.41 (dd, J = 11.8, 7.4 Hz, 1H), 4.37 (d, J = 14.3 Hz, 1H), 4.22 (d, J = 14.2 Hz, 1H), 4.11 (d, J = 3.4 Hz, 1H), 3.87 (s, 3H), 3.79 (s, 3H), 2.91 (td, J = 13.7, 7.4 Hz, 1H), 2.51 (dt, J = 14.8, 3.2 Hz, 1H), 2.26 (dd, J = 14.5, 7.3 Hz, 1H), 1.76 (d, J = 6.8 Hz, 3H), 1.62 – 1.56 (m, 1H). ^{13}C NMR (151 MHz, $CDCl_3$) δ 166.89, 164.68, 142.44, 134.42, 132.20, 129.06, 127.89, 125.86, 114.54, 111.67, 102.09, 72.13, 64.27, 63.04, 55.17, 51.83, 50.12, 40.85, 28.18, 28.04, 13.35. HRMS calculated for $C_{21}H_{21}N_2O_2Br$: $[M + H]^+$: 415.1021 (found); 415.1021 (calcd).

*10-Bromo-N-4-allylakuammicine (**24**).* Prepared from **2** (25.0 mg, 0.06229 mmol) according to General Procedure E using allyl bromide (200 equiv) to yield 31.3 mg of **24** (96%). ^{1}H NMR (600 MHz, $CDCl_3$) δ 8.87 (s, 1H), 8.12 (d, J = 1.9 Hz, 1H), 7.30 (dd, J = 8.3, 1.9 Hz, 1H), 6.75 (d, J = 8.3 Hz, 1H), 6.22 (ddt, J = 17.1, 10.0, 7.3 Hz, 1H), 6.03 – 5.97 (m, 1H), 5.79 (dt, J = 4.0, 2.1 Hz, 1H), 5.12 (dd, J = 12.8, 6.9 Hz, 1H), 5.04 (q, J = 2.4 Hz, 1H), 4.59 (dd, J = 12.7, 7.8 Hz, 1H), 4.41 (td, J = 12.4, 7.4 Hz, 1H), 4.26 (q, J = 14.3 Hz, 2H), 4.13 (s, 1H), 4.05 (dd, J = 11.9, 7.2 Hz, 1H), 3.81 (s, 3H), 2.89 (td, J = 13.7, 7.3 Hz, 1H), 2.72 (dt, J = 15.0, 3.2 Hz, 1H), 2.24 (dd, J = 14.3, 7.2 Hz, 1H), 1.76 – 1.72 (m, 3H), 1.56 (d, J = 14.9 Hz, 1H). ^{13}C NMR (151 MHz, $CDCl_3$) δ 166.82, 163.93, 142.22, 134.58, 132.27, 130.52, 129.48, 128.84, 125.62, 125.32, 114.43, 111.70, 102.31, 70.71, 63.64, 61.95, 60.30, 55.06, 51.80, 40.93, 28.69, 28.21, 13.49. HRMS calculated for $C_{23}H_{26}N_2O_2Br$: $[M + H]^+$: 441.1180 (found); 441.1178 (calcd).

*10-Bromo-N-4-cyclopropylmethylakuammicine (**25**).* Prepared from **2** (25.0 mg, 0.06229 mmol) according to General Procedure E using bromomethyl cyclopropane (25 equiv) to yield 10.4 mg of **25** (31%). ^{1}H NMR (600 MHz, $CDCl_3$) δ 8.14 (d, J = 2.0 Hz, 1H), 7.32 (dd, J = 8.3, 1.9 Hz, 1H),

6.75 (d, J = 8.3 Hz, 1H), 5.85 (q, J = 7.3 Hz, 1H), 5.05 (s, 1H), 4.46 (td, J = 12.4, 7.4 Hz, 1H), 4.36 (d, J = 5.7 Hz, 2H), 4.32 (dd, J = 12.9, 7.2 Hz, 1H), 4.24 – 4.20 (m, 1H), 4.14 (s, 1H), 3.91 (dd, J = 13.1, 6.9 Hz, 1H), 3.81 (s, 3H), 2.93 (td, J = 13.8, 7.2 Hz, 1H), 2.65 (dt, J = 15.0, 3.2 Hz, 1H), 2.27 (dd, J = 14.3, 7.2 Hz, 1H), 1.75 (d, J = 6.9 Hz, 3H), 1.57 (d, J = 14.9 Hz, 1H), 1.28 – 1.24 (m, 1H), 0.88 (t, J = 6.4 Hz, 3H). ^{13}C NMR (151 MHz, $CDCl_3$) δ 166.88, 164.12, 142.28, 134.68, 132.34, 129.43, 128.88, 125.63, 114.53, 111.75, 102.33, 71.16, 65.91, 61.63, 60.59, 55.09, 51.85, 41.16, 28.72, 28.31, 13.53, 5.88, 5.30, 5.09. HRMS calculated for $C_{24}H_{28}N_2O_2Br$: $[M + H]^+$: 455.1331 (found); 455.1334 (calcd).

*10-Bromo-19R,20R-dihydroxyakuammicine (**26**).* Prepared from **2** according to General Procedure C to yield 27.6 mg of **26** (46%).^{1}H NMR (600 MHz, $CDCl_3$) δ 9.08 (s, 1H), 7.28 (d, J = 2.0 Hz, 1H), 7.23 (dd, J = 8.2, 2.0 Hz, 1H), 6.68 (d, J = 8.2 Hz, 1H), 3.81 (d, J = 3.2 Hz, 1H), 3.76 (s, 3H), 3.56 (q, J = 6.2 Hz, 1H), 3.10 – 3.03 (m, 2H), 2.97 (t, J = 2.6 Hz, 1H), 2.93 – 2.82 (m, 2H), 2.71 (dt, J = 13.4, 3.2 Hz, 1H), 2.45 (d, J = 13.0 Hz, 1H), 1.87 (dd, J = 13.4, 6.7 Hz, 1H), 1.39 (d, J = 6.2 Hz, 3H), 1.13 (dt, J = 13.2, 3.0 Hz, 1H). ^{13}C NMR (151 MHz, $CDCl_3$) δ 171.06, 168.25, 143.25, 137.79, 130.49, 123.28, 113.45, 111.21, 101.42, 73.52, 72.79, 60.38, 56.76, 54.10, 52.61, 51.34, 42.97, 34.31, 26.24, 17.76. HRMS calculated for $C_{20}H_{24}N_2O_4Br$: $[M + H]^+$: 435.0924 (found); 435.0919 (calcd).

*10-Bromo-19,20-dihydroakuammicine (**27**).* Prepared from **13** (20.20 mg, 0.062 mmol) using General Procedure A to yield 8.6 mg of **27** (42%). ^{1}H NMR (600 MHz, $CDCl_3$) δ 9.03 (s, 1H), 7.25 (d, J = 2.0 Hz, 1H), 7.22 (dd, J = 8.2, 1.9 Hz, 1H), 6.67 (d, J = 8.2 Hz, 1H), 3.86 (d, J = 3.8 Hz, 1H), 3.75 (s, 3H), 3.17 – 3.13 (m, 1H), 3.10 – 3.03 (m, 1H), 2.97 – 2.90 (m, 2H), 2.85 (dd, J = 11.6, 7.2 Hz, 1H), 2.09 – 1.96 (m, 2H), 1.85 (dd, J = 13.4, 6.7 Hz, 1H), 1.70 (s, 1H), 1.40 – 1.33 (m, 2H), 1.06 – 0.98 (m, 1H), 0.97 (t, J = 7.1 Hz, 3H). ^{13}C NMR (151 MHz, $CDCl_3$) δ 170.51, 168.94, 143.65, 137.84, 130.41, 123.23, 113.23, 111.12, 99.66, 61.27, 56.50, 54.15, 51.41, 51.28,

43.15, 39.40, 31.53, 31.04, 26.24, 11.82. HRMS calculated for $C_{20}H_{24}N_2O_2Br$: $[M + H]^+$: 405.0997 (found); 405.0995 (calcd).

In vitro Pharmacology

Drugs. Dimethyl sulfoxide (DMSO), forskolin, [D-Ala2, N-Me-Phe4, Gly5-ol]-Enkephalin acetate salt (DAMGO), and trans-(±)-3,4-dichloro-n-methyl-N-(2-(1 pyrrolidinyl cyclohexyl)benzeneacetamide methanesulfonate (U50,488) were purchased from Sigma-Aldrich (St. Louis, MO, United States). [^{3}H]DAMGO (53.7 Ci/mmol, lot#2376538; 51.7 Ci/mmol, lot#2815607) and [3H]U69,593 (60 Ci/mmol, lot#2367921 and lot#2644168; 49.2 Ci/mmol, lot#2791786) were purchased from PerkinElmer (Waltham, MA, United States).

*Cell Lines and Cell Culture***.** To perform the HiHunter cAMP accumulation assay, Chinese hamster ovary cells (CHO-K1) stably expressing human μ-opioid receptor (OPRM1, catalog no. 95-0107C2, DiscoverX, Fremont, CA, USA) and κ-opioid receptor (OPRK1, catalog no. 95-0088C2, DiscoverX, Fremont, CA, USA) were maintained at 80% confluence in F-12 media supplemented with 10% fetal bovine serum, 1% penicillin/streptomycin/L-glutamine, and 800 μg/mL G418. To perform the PathHunter β-arrestin-2 recruitment assay, U2OS-human κ opioid receptor (κOR) cells stably expressing the κOR and β-arrestin-2 (RRID:CVCL_LA97, DiscoverX, Fremont, CA, USA) were maintained in McCoy's 5A media supplemented with 10% FBS and containing 500 μg/mL geneticin and 250 μg/mL hygromycin. All cells were grown 37 °C under 5% CO_2 in a humidified incubator under sterile conditions in T75 flasks. During passaging, cells were dislodged from the flask following a 3-5 min incubation with 0.25% trypsin or non-enzymatic detachment reagent and subcultivated at ratios of 1:10 (CHO) and 3:10 (U2OS).

HitHunter cAMP Accumulation Assay. CHO-K1 OPRM1 and OPRK1 cells (DiscoverX, Fremont, CA, USA) were maintained with F-12 media until 70 - 80% confluent. When confluent, cells were plated at a concentration of 10,000 cells/well in Assay Complete Plating Reagent (Eurofins) on a 384-well tissue culture plate. The cells were incubated at 37°C under 5% CO_2 in a humidified incubator for 24 hours. 10 mM ligand stock solutions of all ligands were created in DMSO and used to serially dilute in 100% DMSO (100X). Assay buffer (HBSS + 10 mM HEPES) was used to dilute the 100X DMSO dilutions to 10X. Assay buffer with forskolin (0.02 mM) was used to dilute the 10X dilutions to a 5X working concentrations. The HitHunter cAMP Assay for Small Molecules (Eurofins) was used according to manufacturer's instructions to measure the cAMP inhibition of the 5X ligand dilutions in triplicate. Luminescence was quantified using a FlexStation 3 Multi-Mode Microplate reader (Molecular Devices).

PathHunter β-arrestin-2 Recruitment Assay. The β-arrestin-2 recruitment assay was performed using U2OS-human (κOR) PathHunter β-arrestin-2 cells (DiscoverX) as previously described.[74]

Competitive Radioligand Binding. Cell membranes were isolated from CHO and U2OS cells which stably express the μOR and the κOR, respectfully (DiscoverX). The competitive radioligand binding assay was performed on the membrane preparations as previously described with using tritiated radioligands [^{3}H]DAMGO and [^{3}H]U69,593 for the μOR and the κOR, respectfully.[75]

Statistics. Cellular pharmacological data was analyzed using GraphPad 9 (GraphPad Prism software, La Jolla, CA, United States) and is presented as mean ± SEM. Composite figures are representative curves averaged from a minimum of three independent assays which were normalized to vehicle, forskolin, and ligand controls.

Computational

Structure alignment and refinement. The LigPrep feature in Maestro (Schrödinger Suite, 2023-1) was used to compute possible conformation of **5** at pH=7.2 using the OPLS4 force field. The conformation of **5** bearing a protonated nitrogen was aligned to MOM-SalB bound to the κOR (PDB: 8DZP), which had previously been prepared using the Protein Preparation feature. Using the superposition feature, the furan ring and ester of **5** were overlayed onto the furan ring and ester of MOM-SalB. A ligand-receptor complex was formed by replacing MOM-SalB with **5**, and the resulting complex was refined with Prime using the VSGB solvation model, OPLS4 force field, and hierarchal sampling algorithm. Atoms within 5.0 Å of the ligand were refined.

ASSOCIATED CONTENT

Supporting Information

The following files are available free of charge.

Additional supplementary figures (S1-2) and tables (S1-2).

^{1}H NMR and ^{13}C NMR spectra for all synthesized compounds.

AUTHOR INFORMATION

Corresponding Author

*Andrew P. Riley – Department of Pharmaceutical Sciences, College of Pharmacy, University of Illinois at Chicago, Chicago, Illinois 60612, United States. Email: apriley@uic.edu

Author Contributions

The manuscript was written through contributions of all authors. All authors have given approval to the final version of the manuscript.

ACKNOWLEDGEMENTS

We would like to thank Dr. Alexander R. French for assistance with in vitro assays. This work was supported in part by NIH Grants R35GM147005 (APR), DA045897 (RvR), AA025368 (RvR), AA026949 (RvR), T32 Training Grant T32AT007533 (MRH), and a predoctoral fellowship from the American Foundation for Pharmaceutical Education (AMR).

References:

(1) Pathan, H.; Williams, J. Basic Opioid Pharmacology: An Update. *Br J Pain* **2012**, *6*, 11–16.

(2) Valentino, R. J.; Volkow, N. D. Untangling the Complexity of Opioid Receptor Function. *Neuropsychopharmacol* **2018**, *43*, 2514–2520.

(3) James, A.; Williams, J. Basic Opioid Pharmacology — An Update. *Br J Pain* **2020**, *14*, 115–121.

(4) Pasternak, G. W.; Pan, Y.-X. Mu Opioids and Their Receptors: Evolution of a Concept. *Pharmacol Rev.* **2013**, *65*, 1257–1317.

(5) Presley, C. C.; Lindsley, C. W. DARK Classics in Chemical Neuroscience: Opium, a Historical Perspective. *ACS Chem Neurosci* **2018**, *9* (10), 2503–2518.

(6) Darcq, E.; Kieffer, B. L. Opioid Receptors: Drivers to Addiction? *Nat Rev Neurosci* **2018**, *19* (8), 499–514.

(7) Pergolizzi, J. V.; Varrassi, G.; Paladini, A.; LeQuang, J. Stopping or Decreasing Opioid Therapy in Patients on Chronic Opioid Therapy. *Pain Ther* **2019**, *8*, 163–176.

(8) Butelman, E. R.; Yuferov, V.; Kreek, M. J. κ-Opioid Receptor/Dynorphin System: Genetic and Pharmacotherapeutic Implications for Addiction. *Trends Neurosci* **2012**, *35*, 587–596.

(9) Knoll, A. T.; Carlezon, W. A. Dynorphin, Stress, and Depression. *Brain Res* **2010**, *1314*, 56–73.

(10) Millan, M. J. κ-Opioid Receptors and Analgesia. *Trends Pharmacol Sci* **1990**, *11*, 70–76.

(11) Dalefield, M. L.; Scouller, B.; Bibi, R.; Kivell, B. M. The Kappa Opioid Receptor: A Promising Therapeutic Target for Multiple Pathologies. *Front Pharmacol* **2022**, *13*, 837671.

(12) Dunn, A. D.; Reed, B.; Erazo, J.; Ben-Ezra, A.; Kreek, M. J. Signaling Properties of Structurally Diverse Kappa Opioid Receptor Ligands: Toward in Vitro Models of in Vivo Responses. *ACS Chem Neurosci* **2019**, *10*, 3590–3600.

(13) Wadenberg, M.-L. G. A Review of the Properties of Spiradoline: A Potent and Selective k-Opioid Receptor Agonist. *CNS Drug Rev* **2003**, *9*, 187–198.

(14) Schattauer, S. S.; Kuhar, J. R.; Song, A.; Chavkin, C. Nalfurafine Is a G-Protein Biased Agonist Having Significantly Greater Bias at the Human than Rodent Form of the Kappa Opioid Receptor. *Cell Signal* **2017**, *32*, 59–65.

(15) Rives, M.-L.; Rossillo, M.; Liu-Chen, L.-Y.; Javitch, J. A. 6′-Guanidinonaltrindole (6′-GNTI) Is a G Protein-Biased κ-Opioid Receptor Agonist That Inhibits Arrestin Recruitment. *J Biol Chem* **2012**, *287*, 27050–27054.

(16) Munro, T. A.; Duncan, K. K.; Xu, W.; Wang, Y.; Liu-Chen, L.-Y.; Carlezon, W. A.; Cohen, B. M.; Béguin, C. Standard Protecting Groups Create Potent and Selective κ Opioids: Salvinorin B Alkoxymethyl Ethers. *Bioorg Med Chem* **2008**, *16*, 1279–1286.

(17) Frankowski, K. J.; Hedrick, M. P.; Gosalia, P.; Li, K.; Shi, S.; Whipple, D.; Ghosh, P.; Prisinzano, T. E.; Schoenen, F. J.; Su, Y.; Vasile, S.; Sergienko, E.; Gray, W.; Hariharan, S.; Milan, L.; Heynen-Genel, S.; Mangravita-Novo, A.; Vicchiarelli, M.; Smith, L. H.; Streicher, J. M.; Caron, M. G.; Barak, L. S.; Bohn, L. M.; Chung, T. D. Y.; Aubé, J. Discovery of Small Molecule Kappa Opioid Receptor Agonist and Antagonist Chemotypes through a HTS and Hit Refinement Strategy. *ACS Chem Neurosci* **2012**, *3*, 221–236.

(18) Fugal, J.; Serpa, S. M. Difelikefalin: A New κ-Opioid Receptor Agonist for the Treatment of Hemodialysis-Dependent Chronic Kidney Disease–Associated Pruritus. *Ann Pharmacother* **2023**, *57*, 480–488.

(19) Pfeiffer, A.; Brantl, V.; Herz, A.; Emrich, H. M. Psychotomimesis Mediated by κ Opiate Receptors. *Science* **1986**, *233*, 774–776.

(20) Ranganathan, M.; Schnakenberg, A.; Skosnik, P. D.; Cohen, B. M.; Pittman, B.; Sewell, R. A.; D'Souza, D. C. Dose-Related Behavioral, Subjective, Endocrine, and Psychophysiological Effects of the κ Opioid Agonist Salvinorin A in Humans. *Biol Psych* **2012**, *72*, 871–879.

(21) Tejeda, H. A.; Counotte, D. S.; Oh, E.; Ramamoorthy, S.; Schultz-Kuszak, K. N.; Bäckman, C. M.; Chefer, V.; O'Donnell, P.; Shippenberg, T. S. Prefrontal Cortical Kappa-Opioid Receptor Modulation of Local Neurotransmission and Conditioned Place Aversion. *Neuropsychopharmacol* **2013**, *38*, 1770–1779.

(22) Fishbane, S.; Mathur, V.; Germain, M. J.; Shirazian, S.; Bhaduri, S.; Munera, C.; Spencer, R. H.; Menzaghi, F.; Aaronson, M.; Alford, K.; Awad, A.; Bhat, P.; Broumand, V.; Calhoun, W.; Darwish, R.; Dua, S.; Dukes, C.; Erinle, A.; Hadley, A.; Hsieh, J.; Kashif, M.; Kopyt, N.; Kumar, J.; Kusnir, J.; Lee, J.; Maasarani, E.; Miller, R.; Mizani, M. R.; Navarro, J.; Podoll, A.; Pohlman, T.; Rivers, D.; Robinson, D.; Rich, L.; Shirazian, S.; Silva, A.; Smith, M.; Topf, J.; Tumlin, J.; Ungar, S.; Zeig, S. Randomized Controlled Trial of Difelikefalin for Chronic Pruritus in Hemodialysis Patients. *Kidney Int Rep* **2020**, *5*, 600–610.

(23) Zhang, P.; Xiang, S.; Liu, B.; Wang, X.; Yang, X.; Ye, C.; Wang, Z.; Li, Y.; Zhou, L.; Wang, C.; Li, H.; Huang, J.; Peng, A.; Wang, X.; Wang, D.; Xiao, J.; Chen, W.; Cheng, H.; Mao, N.; Wang, J.; Yang, L.; Chen, J. Randomized Controlled Trial of Nalfurafine for Refractory Pruritus in Hemodialysis Patients. *Ren Fail 45*, 2175590.

(24) Bruchas, M. R.; Chavkin, C. Kinase Cascades and Ligand-Directed Signaling at the Kappa Opioid Receptor. *Psychopharmacol (Berl.)* **2010**, *210*, 137–147.

(25) Land, B. B.; Bruchas, M. R.; Schattauer, S.; Giardino, W. J.; Aita, M.; Messinger, D.; Hnasko, T. S.; Palmiter, R. D.; Chavkin, C. Activation of the Kappa Opioid Receptor in the Dorsal Raphe Nucleus Mediates the Aversive Effects of Stress and Reinstates Drug Seeking. *Proc Natl Acad Sci* **2009**, *106*, 19168–19173.

(26) Ehrich, J. M.; Messinger, D. I.; Knakal, C. R.; Kuhar, J. R.; Schattauer, S. S.; Bruchas, M. R.; Zweifel, L. S.; Kieffer, B. L.; Phillips, P. E. M.; Chavkin, C. Kappa Opioid Receptor-Induced Aversion Requires P38 MAPK Activation in VTA Dopamine Neurons. *J Neurosci* **2015**, *35*, 12917–12931.

(27) Bruchas, M. R.; Schindler, A. G.; Shankar, H.; Messinger, D. I.; Miyatake, M.; Land, B. B.; Lemos, J. C.; Hagan, C. E.; Neumaier, J. F.; Quintana, A.; Palmiter, R. D.; Chavkin, C. Selective P38α MAPK Deletion in Serotonergic Neurons Produces Stress Resilience in Models of Depression and Addiction. *Neuron* **2011**, *71*, 498–511.

(28) Bruchas, M. R.; Land, B. B.; Aita, M.; Xu, M.; Barot, S. K.; Li, S.; Chavkin, C. Stress-Induced P38 Mitogen-Activated Protein Kinase Activation Mediates κ-Opioid-Dependent Dysphoria. *J Neurosci* **2007**, *27*, 11614–11623.

(29) Mores, K. L.; Cummins, B. R.; Cassell, R. J.; van Rijn, R. M. A Review of the Therapeutic Potential of Recently Developed G Protein-Biased Kappa Agonists. *Front Pharmacol* **2019**, *10*, 407.

(30) French, A. R.; van Rijn, R. M. An Updated Assessment of the Translational Promise of G-Protein-Biased Kappa Opioid Receptor Agonists to Treat Pain and Other Indications without Debilitating Adverse Effects. *Pharmacol Res* **2022**, *177*, 106091.

(31) White, K. L.; Robinson, J. E.; Zhu, H.; DiBerto, J. F.; Polepally, P. R.; Zjawiony, J. K.; Nichols, D. E.; Malanga, C. J.; Roth, B. L. The G Protein–Biased κ-Opioid Receptor Agonist RB-64 Is Analgesic with a Unique Spectrum of Activities In Vivo. *J Pharmacol Exp Ther* **2015**, *352*, 98–109.

(32) El Daibani, A.; Paggi, J. M.; Kim, K.; Laloudakis, Y. D.; Popov, P.; Bernhard, S. M.; Krumm, B. E.; Olsen, R. H. J.; Diberto, J.; Carroll, F. I.; Katritch, V.; Wünsch, B.; Dror, R. O.; Che, T. Molecular Mechanism of Biased Signaling at the Kappa Opioid Receptor. *Nat Commun* **2023**, *14*, 1338.

(33) Chakraborty, S.; Majumdar, S. Natural Products for the Treatment of Pain: Chemistry and Pharmacology of Salvinorin A, Mitragynine, and Collybolide. *Biochemistry* **2021**, *60*, 1381–1400.

(34) Turnaturi, R.; Piana, S.; Spoto, S.; Costanzo, G.; Reina, L.; Pasquinucci, L.; Parenti, C. From Plant to Chemistry: Sources of Active Opioid Antinociceptive Principles for Medicinal Chemistry and Drug Design. *Molecules* **2023**, *28*, 7089.

(35) Creed, S. M.; Gutridge, A. M.; Argade, M. D.; Hennessy, M. R.; Friesen, J. B.; Pauli, G. F.; Van Rijn, R. M.; Riley, A. P. Isolation and Pharmacological Characterization of Six Opioidergic *Picralima nitida* Alkaloids. *J Nat Prod* **2021**, *84*, 71–80.

(36) Hennessy, M. R.; Gutridge, A. M.; French, A. R.; Rhoda, E. S.; Meqbil, Y. J.; Gill, M.; Kashyap, Y.; Appourchaux, K.; Paul, B.; Wang, Z. J.; van Rijn, R. M.; Riley, A. P. Modified Akuamma Alkaloids with Increased Potency at the Mu-Opioid Receptor. *J Med Chem* **2023**, *66*, 3312–3326.

(37) Wang, J.; Li, R.; Dong, Z.; Liu, P.; Dong, G. Complementary Site-Selectivity in Arene Functionalization Enabled by Overcoming the Ortho Constraint in Palladium/Norbornene Catalysis. *Nat Chem* **2018**, *10*, 866–872.

(38) Váradi, A.; Marrone, G. F.; Palmer, T. C.; Narayan, A.; Szabó, M. R.; Le Rouzic, V.; Grinnell, S. G.; Subrath, J. J.; Warner, E.; Kalra, S.; Hunkele, A.; Pagirsky, J.; Eans, S. O.; Medina, J. M.; Xu, J.; Pan, Y.-X.; Borics, A.; Pasternak, G. W.; McLaughlin, J. P.; Majumdar, S. Mitragynine/Corynantheidine Pseudoindoxyls As Opioid Analgesics with Mu Agonism and Delta Antagonism, Which Do Not Recruit β-Arrestin-2. *J Med Chem* **2016**, *59*, 8381–8397.

(39) Zhu, S.-F.; Yu, Y.-B.; Li, S.; Wang, L.-X.; Zhou, Q.-L. Enantioselective Hydrogenation of α-Substituted Acrylic Acids Catalyzed by Iridium Complexes with Chiral Spiro Aminophosphine Ligands. *Angew Chem Int Ed* **2012**, *51*, 8872–8875.

(40) Teijaro, C. N.; Munagala, S.; Zhao, S.; Sirasani, G.; Kokkonda, P.; Malofeeva, E. V.; Hopper-Borge, E.; Andrade, R. B. Synthesis and Biological Evaluation of Pentacyclic *Strychnos*

Alkaloids as Selective Modulators of the ABCC10 (MRP7) Efflux Pump. *J Med Chem* **2014**, *57*, 10383–10390.

(41) Kokkonda, P.; Brown, K. R.; Seguin, T. J.; Wheeler, S. E.; Vaddypally, S.; Zdilla, M. J.; Andrade, R. B. Biomimetic Total Syntheses of (−)-Leucoridines A and C through the Dimerization of (−)-Dihydrovalparicine. *Angew Chem Int Ed* **2015**, *54*, 12632–12635.

(42) Munagala, S.; Sirasani, G.; Kokkonda, P.; Phadke, M.; Krynetskaia, N.; Lu, P.; Sharom, F. J.; Chaudhury, S.; Abdulhameed, M. D. M.; Tawa, G.; Wallqvist, A.; Martinez, R.; Childers, W.; Abou-Gharbia, M.; Krynetskiy, E.; Andrade, R. B. Synthesis and Evaluation of *Strychnos* Alkaloids as MDR Reversal Agents for Cancer Cell Eradication. *Bioorg Med Chem.* **2014**, *22*, 1148–1155.

(43) Olson, K. M.; Duron, D. I.; Womer, D.; Fell, R.; Streicher, J. M. Comprehensive Molecular Pharmacology Screening Reveals Potential New Receptor Interactions for Clinically Relevant Opioids. *PLoS ONE* **2019**, *14*, e0217371.

(44) Peng, X.; Knapp, B. I.; Bidlack, J. M.; Neumeyer, J. L. Pharmacological Properties of Bivalent Ligands Containing Butorphan Linked to Nalbuphine, Naltrexone, and Naloxone at μ, δ, and κ Opioid Receptors. *J Med Chem* **2007**, *50*, 2254–2258.

(45) Martin-Flores, M.; Singh, B.; Walsh, C. A.; Brooks, E. P.; Taylor, L. C.; Mitchell, L. M. Effects of Buprenorphine, Methylnaltrexone, and Their Combination on Gastrointestinal Transit in Healthy New Zealand White Rabbits. *J Am Assoc Lab Anim Sci* **2017**, *56*, 155–159.

(46) Bluhm, L. H.; Li, T. Chromatographic Purification of Quaternary Ammonium and Pyridinium Compounds on Normal Phase Silica Gel. *Tet Lett* **1998**, *39*, 3623–3626.

(47) Brust, T. F.; Morgenweck, J.; Kim, S. A.; Rose, J. H.; Locke, J. L.; Schmid, C. L.; Zhou, L.; Stahl, E. L.; Cameron, M. D.; Scarry, S. M.; Aubé, J.; Jones, S. R.; Martin, T. J.; Bohn, L. M. Biased Agonists of the Kappa Opioid Receptor Suppress Pain and Itch without Causing Sedation or Dysphoria. *Sci Signal* **2016**, *9*, 117

(48) Dunn, A. D.; Reed, B.; Guariglia, C.; Dunn, A. M.; Hillman, J. M.; Kreek, M. J. Structurally Related Kappa Opioid Receptor Agonists with Substantial Differential Signaling Bias: Neuroendocrine and Behavioral Effects in C57BL6 Mice. *Int J Neuropsychopharmacol* **2018**, *21*, 847–857.

(49) Smith, J. S.; Lefkowitz, R. J.; Rajagopal, S. Biased Signalling: From Simple Switches to Allosteric Microprocessors. *Nat Rev Drug Discov* **2018**, *17*, 243–260.

(50) Szpakowska, M.; Decker, A. M.; Meyrath, M.; Palmer, C. B.; Blough, B. E.; Namjoshi, O. A.; Chevigné, A. The Natural Analgesic Conolidine Targets the Newly Identified Opioid Scavenger ACKR3/CXCR7. *Signal Transduct Target Ther* **2021**, *6*, 1–3.

(51) Chakraborty, S.; Uprety, R.; Slocum, S. T.; Irie, T.; Le Rouzic, V.; Li, X.; Wilson, L. L.; Scouller, B.; Alder, A. F.; Kruegel, A. C.; Ansonoff, M.; Varadi, A.; Eans, S. O.; Hunkele, A.; Allaoa, A.; Kalra, S.; Xu, J.; Pan, Y. X.; Pintar, J.; Kivell, B. M.; Pasternak, G. W.; Cameron, M. D.; McLaughlin, J. P.; Sames, D.; Majumdar, S. Oxidative Metabolism as a Modulator of Kratom's Biological Actions. *J Med Chem* **2021**, *64*, 16553–16572.

(52) Meyrath, M.; Szpakowska, M.; Zeiner, J.; Massotte, L.; Merz, M. P.; Benkel, T.; Simon, K.; Ohnmacht, J.; Turner, J. D.; Krüger, R.; Seutin, V.; Ollert, M.; Kostenis, E.; Chevigné, A. The Atypical Chemokine Receptor ACKR3/CXCR7 Is a Broad-Spectrum Scavenger for Opioid Peptides. *Nat Commun* **2020**, *11*, 3033.

(53) Kroeze, W. K.; Sassano, M. F.; Huang, X.-P.; Lansu, K.; McCorvy, J. D.; Giguère, P. M.; Sciaky, N.; Roth, B. L. PRESTO-Tango as an Open-Source Resource for Interrogation of the Druggable Human GPCRome. *Nat Struct Mol Biol* **2015**, *22*, 362–369.

(54) Erharuyi, O.; Falodun, A.; Langer, P. Medicinal Uses, Phytochemistry and Pharmacology of *Picralima nitida* (Apocynaceae) in Tropical Diseases: A Review. *Asian Pac J Trop Med* **2014**, *7*, 1–8.

(55) Dapaah, G.; Koffuor, G. A.; Mante, P. K.; Ben, I. O. Antitussive, Expectorant and Analgesic Effects of the Ethanol Seed Extract of *Picralima nitida* (Stapf) Th. & H. Durand. *Res Pharm Sci* **2016**, *11*, 100–112.

(56) Duwiejua, M.; Woode, E.; Obiri, D. D. Pseudo-Akuammigine, an Alkaloid from *Picralima nitida* Seeds, Has Anti-Inflammatory and Analgesic Actions in Rats. *J Ethnopharmacol* **2002**, *81*, 73–79.

(57) Woode, E.; Obiri, D.; Ansah, C.; Duwiejua, M. Total Alkaloidal Extract of *Picralima nitida* (Fam. Apocynaceae) Seeds Has Anti-Inflammatory Actions. *J Ghana Sci Assoc* **2006**, *8*, 70–78.

(58) Lewin, G.; Le Ménez, P.; Rolland, Y.; Renouard, A.; Giesen-Crouse, E. Akuammine and Dihydroakuammine, Two Indolomonoterpene Alkaloids Displaying Affinity for Opioid Receptors. *J Nat Prod* **1992**, *55*, 380–384.

(59) Levy, J.; Le Men, J.; Janot, M. M. Akuammicine, an Alkaloid from the Seeds of *Picralima nitida*. *Bull Soc Chim Fr* **1960**, 979–981.

(60) Menzies, J. R. W.; Paterson, S. J.; Duwiejua, M.; Corbett, A. D. Opioid Activity of Alkaloids Extracted from *Picralima nitida* (Fam. Apocynaceae). *Eur J Pharmacol* **1998**, *350*, 101–108.

(61) Zhou, L.; Lovell, K. M.; Frankowski, K. J.; Slauson, S. R.; Phillips, A. M.; Streicher, J. M.; Stahl, E.; Schmid, C. L.; Hodder, P.; Madoux, F.; Cameron, M. D.; Prisinzano, T. E.; Aubé, J.; Bohn, L. M. Development of Functionally Selective, Small Molecule Agonists at Kappa Opioid Receptors. *J Biol Chem* **2013**, *288*, 36703–36716.

(62) Von Voigtlander, P. F.; Lewis, R. A. U-50,488, a Selective Kappa Opioid Agonist: Comparison to Other Reputed Kappa Agonists. *Prog Neuropsychopharmacol Biol Psych* **1982**, *6*, 467–470.

(63) Han, J.; Zhang, J.; Nazarova, A. L.; Bernhard, S. M.; Krumm, B. E.; Zhao, L.; Lam, J. H.; Rangari, V. A.; Majumdar, S.; Nichols, D. E.; Katritch, V.; Yuan, P.; Fay, J. F.; Che, T. Ligand and G-Protein Selectivity in the κ-Opioid Receptor. *Nature* **2023**, *617*, 417–425.

(64) Mafi, A.; Kim, S.-K.; Goddard, W. A. The Atomistic Level Structure for the Activated Human κ-Opioid Receptor Bound to the Full Gi Protein and the MP1104 Agonist. *Proc Natl Acad Sci* **2020**, *117*, 5836–5843.

(65) Vanderah, T. W. Delta and Kappa Opioid Receptors as Suitable Drug Targets for Pain. *Clin J Pain* **2010**, *26*, S10.

(66) Reed, B.; Butelman, E. R.; Kreek, M. J. Kappa Opioid Receptor Antagonists as Potential Therapeutics for Mood and Substance Use Disorders. In *The Kappa Opioid Receptor*; Liu-Chen, L.-Y., Inan, S., Eds.; Springer International Publishing: Cham, 2022; pp 473–491.

(67) Liu, J. J.; Chiu, Y.-T.; DiMattio, K. M.; Chen, C.; Huang, P.; Gentile, T. A.; Muschamp, J. W.; Cowan, A.; Mann, M.; Liu-Chen, L.-Y. Phosphoproteomic Approach for Agonist-Specific Signaling in Mouse Brains: mTOR Pathway Is Involved in κ Opioid Aversion. *Neuropsychopharmacol* **2019**, *44*, 939–949.

(68) Liu-Chen, L.-Y.; Huang, P. Signaling Underlying Kappa Opioid Receptor-Mediated Behaviors in Rodents. *Front Neurosci* **2022**, *16*.

(69) Beck, T. C.; Dix, T. A. Targeting Peripheral κ-Opioid Receptors for the Non-Addictive Treatment of Pain. *Future Drug Discov* **2019**, *1*, FDD17.

(70) Martínez, V.; Abalo, R. Peripherally Acting Opioid Analgesics and Peripherally-Induced Analgesia. *Behav Pharmacol* **2020**, *31*, 136–158.

(71) Husbands, S. M.; Neilan, C. L.; Broadbear, J.; Grundt, P.; Breeden, S.; Aceto, M. D.; Woods, J. H.; Lewis, J. W.; R. Traynor, J. BU74, a Complex Oripavine Derivative with Potent Kappa Opioid Receptor Agonism and Delayed Opioid Antagonism. *Eur J Pharmacol* **2005**, *509*, 117–125.

(72) Huang, W.; Manglik, A.; Venkatakrishnan, A. J.; Laeremans, T.; Feinberg, E. N.; Sanborn, A. L.; Kato, H. E.; Livingston, K. E.; Thorsen, T. S.; Kling, R.; Granier, S.; Gmeiner, P.; Husbands, S. M.; Traynor, J. R.; Weis, W. I.; Steyaert, J.; Dror, R. O.; Kobilka, B. K. Structural Insights into μ-Opioid Receptor Activation. *Nature* **2015**, *524*, 315–321.

(73) Hong, A. Y.; Vanderwal, C. D. A Synthesis of Alsmaphorazine B Demonstrates the Chemical Feasibility of a New Biogenetic Hypothesis. *J Am Chem Soc* **2015**, *137*, 7306–7309.

(74) Chiang, T.; Sansuk, K.; van Rijn, R. M. β-Arrestin 2 Dependence of δ Opioid Receptor Agonists Is Correlated with Alcohol Intake. *Br J Pharmacol* **2016**, *173*, 332–343.

(75) Cassell, R. J.; Mores, K. L.; Zerfas, B. L.; Mahmoud, A. H.; Lill, M. A.; Trader, D. J.; van Rijn, R. M. Rubiscolins Are Naturally Occurring G Protein-Biased Delta Opioid Receptor Peptides. *Eur Neuropsychopharmacol* **2019**, *29*, 450–456.

TOC GRAPHIC